

# Amphibole-bearing metamorphic clasts in ANDRILL AND-2A core: A provenance tool to unravel the Miocene glacial history in the Ross Embayment (western Ross Sea, Antarctica)

Franco M. Talarico<sup>1</sup>, Donato Pace<sup>1</sup>, and Sonia Sandroni<sup>2</sup>

<sup>1</sup>Dipartimento di Scienze della Terra, Università degli Studi di Siena, Via Laterina 8, 53100 Siena, Italy

<sup>2</sup>Museo Nazionale dell'Antartide, Università degli Studi di Siena, Via Laterina 8, 53100 Siena, Italy

## ABSTRACT

A petrological investigation of amphibole-bearing metamorphic clasts in the ANDRILL AND-2A core allows a detailed comparison with similar lithologies from potential source regions, leading to the identification of three distinct provenance areas in the present-day segment of the Transantarctic Mountains between the Byrd Glacier and the Blue Glacier (Mulock-Skelton glacier area, the Britannia Range, and the Koettlitz-Blue glacier area in the Royal Society Range). A key role in the comparison is played by the wide range of Ca-amphibole compositions, type of intracrystalline zoning, mineral assemblages, and fabrics, which reflect different bulk rocks and metamorphic conditions. Ca-amphibole compositions and zonations also offer the opportunity for the application of geothermobarometry methods, which, consistent with literature data, provide further evidence that the three provenance regions correspond to distinct metamorphic terrains with pervasive medium-pressure amphibolite-grade conditions restricted to the Britannia Range. The study contributes new insights into the depositional processes in a variety of glacial environments ranging from open marine with icebergs to distal, proximal, and subglacial settings. The results also highlight the record of two distinct glacial scenarios reflecting either short-range (<100 km) fluctuations of paleoglaciers in the Royal Society Range with dominant flows from W to E, or larger volume of ice sourced from southernmore outlet glaciers from the Skelton-Byrd glacier area with flow lines running N-S close to the Transantarctic Mountains front. Both scenarios demonstrate the importance of the AND-2A core to reveal a hitherto unavail-

able, near-field record of dynamic paleoenvironmental history through the Miocene.

## INTRODUCTION

The ANDRILL Southern McMurdo Sound (SMS) project (Harwood et al., 2008–2009) is the last one of several scientific Antarctic drilling projects (DSDP, DVDP, MSSTS-CIROS, CRP; Hambrey et al., 2002, and references therein; AND-1B, Naish et al., 2007) that recovered significant sections of the latest Eocene to Pleistocene sedimentary succession deposited in the Victoria Land Basin (Cooper and Davey, 1985), a structural half-graben, ~350 km long, bounded on its western side by the Transantarctic Mountains (TAM) front (Barrett, 1979; Wilson, 1999; Fig. 1).

The ANDRILL SMS project drilled the AND-2A drill hole from a site located in the southern part of McMurdo Sound, ~30 km west of McMurdo Station (77°45.488'S; 165°16.613'E) near the termination of Koettlitz and Blue glaciers (Fig. 1). Regional seismic-reflection surveys show that the penetrated succession is composed of a series of clinoform sets produced by uplift and erosion as a result of renewed rifting of the Terror Rift (Fielding et al., 2008). Accommodation for sediment was produced through fault- and flexure-related subsidence associated with rifting. The active rifting and passive thermal subsidence during the early and middle Miocene produced the accommodation for the accumulation of this Neogene succession (Fielding et al., 2008).

With a recovery of ~98%, the AND-2A core recovered an almost 1140-m-long succession including a thick and fairly continuous lower to middle Miocene lower part (~1140–225 mbsf [meters below sea floor]) and an upper part (above 225 mbsf), ranging in age from late Mio-

cene to Pleistocene, which is punctuated by several disconformities, not clearly defined yet but with an accumulative loss of 7–8 m.y. (Harwood et al., 2008–2009; Acton et al., 2008–2009 with modifications as in ANDRILL SMS Science Team, 2010) (Fig. 2). The succession includes several intervals of massive and stratified sandy diamictites (lithofacies 8 and 7, respectively, as defined by Fielding et al., 2008–2009), with variable local internal deformation, fossil content and bioturbation, and mainly interpreted as glaciomarine sediments that accumulated at varying proximity to grounded ice, but almost always at some distance. However, evidences of few and short-lived grounding events are documented above 225 mbsf and below 650 mbsf (Passchier et al., 2010). Other common lithologies include sandstones (lithofacies 5), interstratified siltstone and sandstone (lithofacies 3), siltstone to very fine-grained sandstone (lithofacies 2), and interbedded conglomerate and sandstone (lithofacies 9).

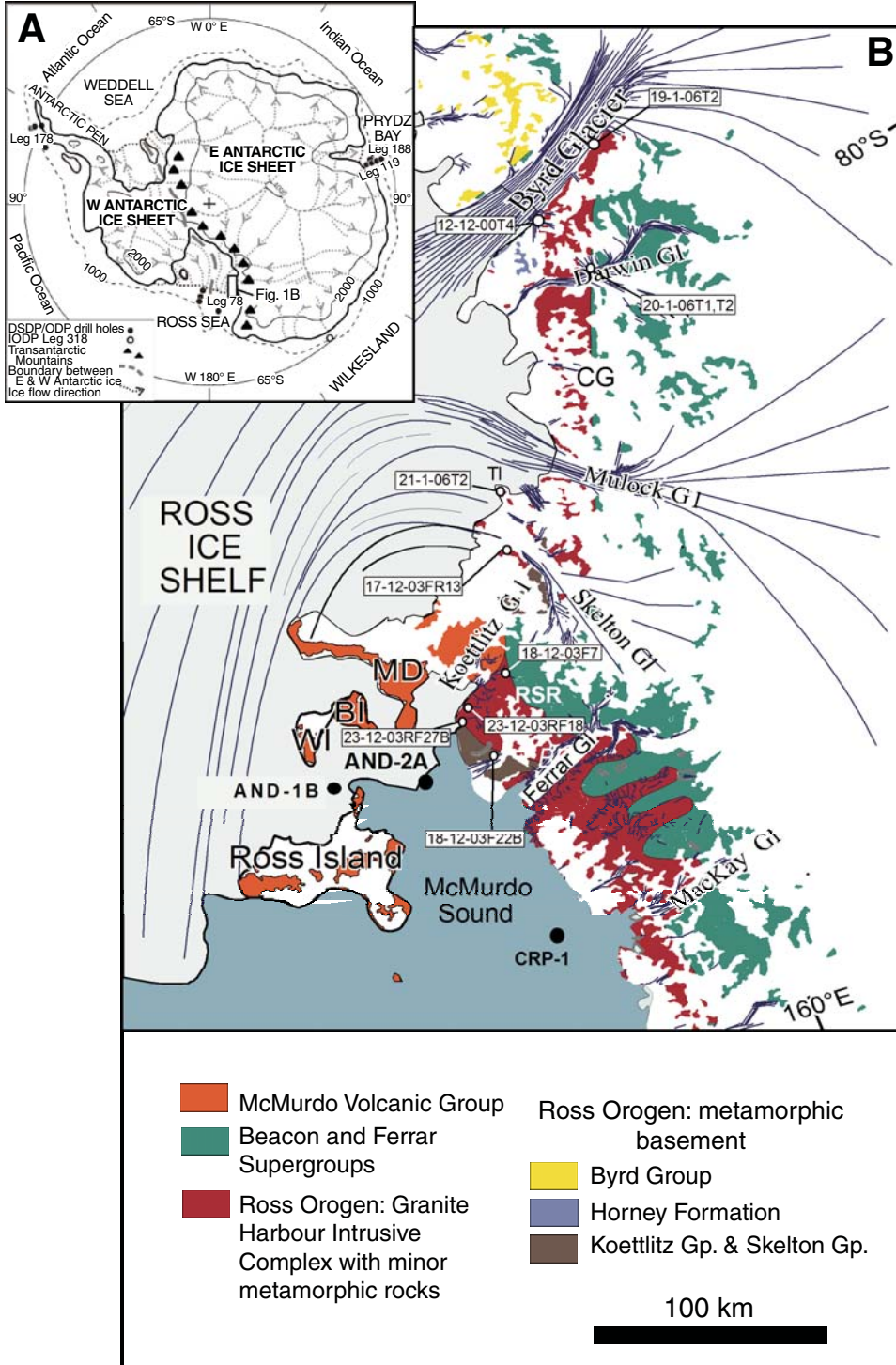
The AND-2A core represents the first thick Miocene section recovered from an ice-proximal setting, and it provides a unique physical record for reconstructing the Antarctic paleoclimatic evolution and the behavior of its ice sheets during the critical climatic events of the late Cenozoic. As demonstrated by several studies in other Victoria Land Basin cored sedimentary sections (e.g., Talarico and Sandroni, 2009) and in glacial successions of the Antarctic continental margin elsewhere (e.g., Reinardy et al., 2009), compositional and distribution patterns of gravel fraction throughout the AND-2A core play a key role in the identification of potential provenance regions and reconstruction of ice-flow patterns. Moreover, distribution patterns and textural analysis of the gravel fraction provide relevant additional information to sedimentological models for subglacial and glacial-marine

depositional settings and processes (e.g., Cowan et al., 2008; Reinardy et al., 2009).

In this paper, we especially concentrate on the provenance history recorded in the clast-rich diamictite units and, subordinately, in other finer-grained lithofacies, and use the detailed petrographical and mineralogical characteris-

tics of a distinctive group of metamorphic clasts (i.e., Ca-amphibole-bearing metasedimentary and metaigneous rocks) to track provenance changes documented in the Miocene to Pliocene AND-2A core section (between 150 and 1140 mbsf). The results are significant for their implications for the glacial evolution recorded

in the Ross Embayment during Miocene time, which, as indicated by proxy records, includes several events of paleoenvironmental changes, such as the mid-Miocene climatic optimum (ca. 17–14 Ma; Billups and Schrag, 2002; Holbourn et al., 2007; You et al., 2009) and the Mi1a and Mi1b glaciations (Miller et al., 1996).



## GEOLOGICAL SETTING

The southern McMurdo Sound is surrounded with terrains characterized with a broad variety of rock types. Late Cenozoic (ca. 19 Ma to recent) alkali volcanic rocks, mainly basanites of the McMurdo Volcanic Group, form several volcanic centers exposed to the south and east of the AND-2A drill site. The emplacement of Ross Island volcanoes resulted in significant modification of the McMurdo Sound paleogeography and flexural loading with related basin subsidence (Kyle, 1981, 1990). In contrast, the Transantarctic Mountains to the west and southwest are composed primarily of late Proterozoic–Cambrian metamorphic rocks (Koettlitz and Skelton Groups, Gunn and Warren, 1962; Findlay et al., 1984; Cook and Craw, 2001, 2002; Horney Formation, Borg et al., 1987) and Cambrian–Ordovician granitoids of the Granite Harbour Intrusive Complex (Gunn and Warren, 1962). In the westernmost part of the Transantarctic Mountains, this basement is unconformably overlain by sedimentary rocks, mainly nonmarine sandstones, quartzites, and siltstones of the Devonian to Triassic Beacon Supergroup (Barrett, 1991). In the Jurassic, sills of the Ferrar Dolerite intruded basement and sedimentary cover contemporaneously with their extrusive equivalent, the Kirkpatrick Basalt (Elliot, 1992; Elliot et al., 1995).

In the region comprised between Byrd and Ferrar glaciers, the crystalline basement consists of a variety of lithologies with prominent changes of both metamorphic grade and granulite fabrics throughout the region (Stump, 1995; Goodge, 2007; Talarico and Sandroni, 2009 and references therein for a detailed description of the most abundant basement lithologies) (Fig. 1). In the Royal Society Range, basement rocks comprise mainly upper amphibolite-grade metasediments and orthogneisses (Koettlitz Group, Findlay et al., 1984), variably deformed granodiorites of the Bonney Pluton (Cox, 1993), minor mafic intrusions and alkaline intrusives (Cooper et al., 1997).

The Mulock-Skelton glacier region is characterized by lower greenschist- to lower amphibolite-facies metasediments of the Skelton Group (Gunn and Warren, 1962; Cook and Craw, 2001) and minor, mainly alkaline type, quartz syenites, and granites (Rowell et al., 1993), including biotite ± hornblende porphyritic varieties (e.g., Teall Island, Mulock Glacier area; Cottle and Cooper, 2006; Carosi et al., 2007).

Farther south, between Darwin Glacier and Byrd Glacier, medium- to high-grade metasediments (banded gneisses, schists with Ca-silicate layers, migmatites, and minor amphibolite and marbles) and variably deformed (foliated to mylonitic) granitoids are common in the Hor-

ney Formation (Carosi et al., 2007). Low-grade metasediments, including extensive exposures of metalimestone and metaconglomerates (Cradock, 1970; Goodge et al., 2004), are the dominant lithologies south of Byrd Glacier (Fig. 1).

## MATERIALS AND METHODS

In the AND-2A core, a total number of 103,759 clasts ranging in size from boulder to granule class (>2 mm) were counted and, for each clast, information such as occurrence depth, lithology, 2-D dimensions, and shape were logged on the cut surface of the working-half core (Panter et al., 2008–2009). A preliminary clast sample collection conducted while on the ice was later enlarged by a more extensive sampling at the Antarctic Marine Geology Research Facility (Florida State University, Tallahassee, U.S.A.), where the AND-2A core boxes are stored.

Petrographical analyses by means of polarized-light microscopy of 530 basement clast samples, distributed throughout the whole AND-2A core interval, allowed the identification and selection of 19 samples, all characterized by Ca-amphibole-bearing mineral assemblages.

Provenance inferences were based on detailed petrographical comparisons of investigated clasts with petrographically similar lithologies sampled in 45 localities in the crystalline basement exposed between Byrd and Ferrar glaciers. The used rock sample collection consists of over 600 samples (comprehensive of both metamorphic and intrusive basement rocks) and thin sections stored at the Italian Antarctic National Museum–Earth Science section in Siena.

A selection of ten samples from outcrops, representative of the most widespread Ca-amphibole-bearing metamorphic rocks, and the 19 clast samples were analyzed for their microstructures and mineral compositions using an X-ray energy-dispersive system (EDAX-DX4) attached to a scanning electron microscope (Philips XL30) at the Dipartimento di Scienze della Terra of Siena (Italy). Analytical conditions were 20 kV of accelerating voltage, 25  $\mu$ A of emission current, and a beam spot size of 0.2  $\mu$ m. Natural minerals were used as standards. In each sample, at least 20 analytical spots from at least four crystals were collected for each mineral. Representative core and rim compositions are listed in Table 3 and the Supplemental Table<sup>1</sup>.

<sup>1</sup>Supplemental Table. Excel file of Chemical Compositions of Representative Ca-Amphiboles in AND-2A Metamorphic Clasts. If you are viewing the PDF of this paper or reading it offline, please visit <http://dx.doi.org/10.1130/GES00653.S1> or the full-text article on [www.gsapubs.org](http://www.gsapubs.org) to view the Supplemental Table.

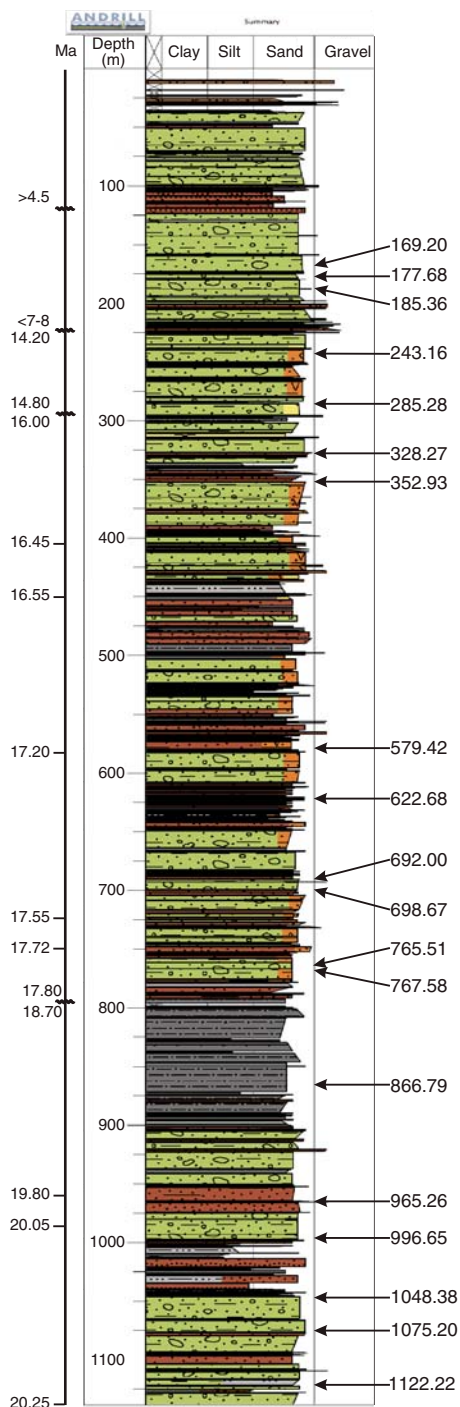


**Figure 2.** Distribution of investigated amphibole-bearing metamorphic clasts in the AND-2A core. Lithology and stratigraphy follow Fielding et al. (2008–2009), Acton et al. (2008–2009, with modifications reported by ANDRILL SMS Science Team, 2010) and Di Vincenzo et al. (2010). Green—diamicrites; brown—sandstones; gray—mudstones; yellow—diatomite; orange—volcaniclastic sediments (including basaltic lava in the uppermost 35 m).

Amphiboles were classified following the nomenclature by Leake et al. (1997); mineral analyses were normalized to 23 oxygens and sum ( $T1 + T2 + M1 + M2 + M3$ ) = 13 as detailed by Triboulet (1992), with  $Fe^{3+}$  estimated as maximum according to Papike et al. (1974).

## RESULTS

### The AND-2A Amphibole-Bearing Metamorphic Clasts: Distribution and Sedimentological Features of the Host Core Intervals

Clast logging and sampling revealed the occurrence of 19 core sections with one or several amphibole-bearing metamorphic clasts, ranging in size from small pebbles to cobbles, and angular to well rounded in shape.

Nineteen samples, one from each core interval characterized by a single homogeneous lithofacies, were selected in this study, the only exception being core interval between 756.19 and 774.94 mbsf where two samples were considered (Fig. 2). The studied clasts are listed in Table 1, together with detailed information concerning their morphological features (dimension and shape), and associated clast assemblages (including clast dimension and shape data) in the core sections corresponding to the specific host lithofacies intervals with top and bottom boundaries as defined by Fielding et al. (2008–2009).

Ca-amphibole-bearing metamorphic clasts are scattered throughout most of the AND-2A core between 166.20 and 1122.22 mbsf, spanning in age from Pliocene–late Miocene ( $>4.5$  Ma,  $<7$ – $8$  Ma) to Early Miocene (ca. 20 Ma) (Table 1).

The size of the analyzed clast samples ranges from 2 to 12 cm (longest axis visible on the cut surface of the working-half core). The degree of roundness is variable, from angular to well rounded, with no evidence of relation between lithology and degree of rounding. Host lithologies include dominant sandy diamictite and minor conglomerates, sandstones, and mudstones. The diamictites occur as units of variable thickness (~1.5–27 m) and, mainly in the core sections above 225 mbsf and below 650 mbsf, they show variable evidence of internal deformation interpreted as indicating subglacial depositional settings (Fielding et al., 2008–2009; Passchier et al., 2010; Table 1).

### Mineralogical Features of Amphibole-Bearing Metamorphic Clasts and Associated Clasts

In the AND-2A core gravel fraction, Ca-amphibole-bearing metamorphic mineral

assemblages occur in a wide range of lithologies including both low-grade metasediments (e.g., metasandstones) and medium-grade rock types (schists, amphibolites, and paragneisses and orthogneisses). Mineral assemblages (type of mineralogical phase and its modal content and composition) and fabric (grain size and type of foliation) show several variations, which consistently reflect the variable metamorphic grade and bulk rock composition (Table 2). Quartz, Ca-amphibole, and plagioclase are commonly accompanied by biotite and K-feldspar. Clinopyroxene is restricted to four samples including a metasandstone, a schist, an orthogneiss, and a Ca-silicate granofels, where the Mg-richest compositions occur. Titanite and opaque minerals are common accessory minerals. Clinzoisite and/or epidote and calcite are rare secondary minerals.

Metasandstones are heterogranular, very fine to fine grained, interlobate granoblastic to granolepidoblastic in texture, with quartzite lithics and detrital mineral grains including subangular quartz and plagioclase. Ca-amphibole poikiloblasts define a spotted texture, most likely as the result of a thermometamorphic overprint (Fig. 3).

Schists are heterogranular, very fine to fine grained, nematogranoblastic, with isoriented amphibole idioblasts (tremolite to green hornblende in composition) and interlobate to subpolygonal plagioclase and quartz; a compositional layering is commonly present.

Paragneisses are heterogranular, fine to medium grained, from interlobate and/or subpolygonal granoblastic to granonematoblastic in texture (Fig. 3), and they are sometimes characterized by compositional layering.

Orthogneisses are heterogranular, fine to medium grained, syenogranitic to tonalitic in composition, with porphyroclastic to mylonitic textures (Fig. 3). The clinopyroxene-bearing variety shows tonalitic composition and is characterized by relict clinopyroxene porphyroclasts and rare green hornblende associated with biotite within the matrix.

Amphibolites are heterogranular, fine grained, nematoblastic, or decussate in texture (Fig. 3). Ca-silicate granofels are heterogranular, very fine to fine grained rocks showing interlobate to subpolygonal granoblastic textures (Fig. 3).

The investigated Ca-amphibole-bearing metamorphic clasts are a minor component of the lithologically varied clast assemblages, which, as reported in Table 1, can be conveniently described in terms of seven main lithological groups, including intrusive, metamorphic, sedimentary, and volcanic rocks, dolerites, quartz (likely derived from intrusive rocks), and intraclasts (coarse sandstones,

diamictites, conglomerates, and minor siltstones; Panter et al., 2008–2009).

In the 19 investigated intervals, the intrusive rock clasts comprise granule to pebble of dominant monzogranites and granodiorites (undeformed to foliated in texture), diorites, gabbros, and tonalites (undeformed to foliated in texture) with minor occurrences of syenogranites, felsic porphyries, and aplites. The metamorphic rocks range in size from granule to cobble and include orthogneisses and paragneisses, granofels, marbles, schists, quartzites, a large variety of low-grade metasediments, and minor metarhyolites, metatonalites, metadiorites, and amphibolites. The sedimentary rocks range in size from granules to pebbles sourced from the Beacon Supergroup (arkose, lithic arkose, and arkosic litharenite; quartz arenite; subarkose) or unknown sources (hybrid and/or mixed arenite, biomicrite and/or wackestone; Cornamusini, 2010). The dolerites include coarse- to fine-grained varieties and show the largest range in the clast size, occurring as granules to cobbles. The volcanic rocks are represented by granule- to cobble-size clasts of lavas ranging from mafic, intermediate to felsic compositions, and from aphanitic to porphyritic and nonvesicular to vesicular in textures (for further details, see Panter et al., 2008–2009; Di Vincenzo et al., 2010).

The occurrence of primary volcanic products, such as pumice and lapilli, was reported at several depths in the investigated core sections (Panter et al., 2008–2009; Di Vincenzo et al., 2010). This clast component was not considered in data analysis; nevertheless, counts of the smaller volcanic clasts could also include some primary volcanic products.

Comparison of clast compositions in the most represented, clast-rich, and lithologically similar core sections (i.e., stratified diamictites) throughout the investigated record indicate prominent differences between diamictite intervals above 774 mbsf (characterized by more abundant and varied basement clast assemblages, and high amounts of Beacon Sandstone and Ferrar Dolerite) and those below 981 mbsf, which show high amounts (60%–95%) of volcanic clasts. The volcanic component is also very important in mudstone-dominated intervals (i.e., 846–872 mbsf) whereas sandstone-rich intervals show variable clast compositions with basement clasts ranging between 25% and 75%.

### Comparison with Potential Source Rock Units and Provenance Implications

Preliminary petrographical investigations (Panter et al., 2008–2009) followed by more detailed petrographical analyses on ~530 clast samples evenly distributed throughout

TABLE 1. SEDIMENTOLOGICAL AND PETROLOGICAL FEATURES OF AND-2A CORE SECTIONS HOSTING THE INVESTIGATED CA-AMPHIBOLE METAMORPHIC CLASTS

| Clast sample | Size (cm) | Shape | Lithology (lithofacies)*   | Hosting interval |                   | Age (Ma)  | Associated clast assemblages |        |     |     |     |             |        |    |     |     | Maximum clast size (cm) |    |
|--------------|-----------|-------|--|------------------|-------------------|-----------|------------------------------|--------|-----|-----|-----|-------------|--------|----|-----|-----|-------------------------|----|
|              |           |       |  | Top depth (mbsf) | Base depth (mbsf) |           | Clast composition (%)        |        |     |     |     | Clast shape |        |    |     |     |                         |    |
|              |           |       |  |                  |                   |           | Met                          | Intrus | Qtz | Sed | Dol | Volc        | Intrac | a  | s-a | s-r |                         | r  |
| 166.20       | 3         | r     | Clast-rich sandy diamicite (8)                                       | 162.58           | 172.90            | >4.5      | 7                            | 30     | 13  | 2   | 5   | 35          | 8      | 15 | x   | x   | x                       | 14 |
| 178.68       | 3         | s-r   | Clast-rich muddy diamicite (8)                                       | 176.28           | 177.98            |           | 3                            | 8      | 11  | 1   | 1   | 75          | 1      | 17 | x   | x   |                         | 11 |
| 185.35       | 12        | r     | Clast-rich sandy diamicite (7)                                       | 181.82           | 187.19            | <7        | 7                            | 34     | 15  | 2   | 6   | 34          | 2      | 27 | x   | x   | x                       | 15 |
| 243.16       | 4         | r     | Volcanic-bearing, clast-rich sandy diamicite (7)                     | 238.89           | 249.83            | ca. 14.45 | 18                           | 45     | 2   | 1   | 6   | 26          | 2      | 15 | x   | x   | x                       | 15 |
| 285.28       | 2         | s-a   | Diatom-bearing, clast-poor sandy diamicite (7)                       | 284.42           | 288.30            | ca. 14.80 | 8                            | 34     |     | 1   | 18  | 39          |        | 5  | x   | x   | x                       | 7  |
| 328.27       | 1         | s-r   | Siltstone and fine sandstone with dispersed clasts (5)               | 328.10           | 328.36            | ca. 15.90 | 25                           | 50     |     |     | 25  |             |        | 2  | x   | x   | x                       | 3  |
| 352.93       | 4         | s-a   | Volcanic-bearing, fine to medium sandstone with dispersed clasts (5) | 352.90           | 353.24            | ca. 16.45 | 8                            | 22     |     | 2   | 68  |             |        | 2  |     | x   | x                       | 3  |
| 579.42       | 2         | s-a   | Volcanic-bearing, clast-poor sandy diamicite (7)                     | 579.33           | 580.97            | ca. 17.20 | 4                            | 19     | 10  |     | 5   | 62          |        | 9  | x   | x   | x                       | 9  |
| 622.68       | 2         | a     | Volcanic-bearing, fine to medium sandstone with dispersed clasts (5) | 621.20           | 622.80            |           | 2                            | 18     | 3   | 1   | 4   | 68          | 4      | 5  | x   | x   | x                       | 4  |
| 692.00       | 5         | r     | Clast-poor sandy diamicite (7)                                       | 681.92           | 692.08            |           | 6                            | 37     |     | 2   | 19  | 36          |        | 9  | x   | x   | x                       | 7  |
| 698.67       | 3         | s-r   | Clast-poor sandy diamicite (7)                                       | 692.89           | 699.02            | 17.55     | 3                            | 22     | 14  | 3   | 10  | 48          |        | 7  | x   | x   |                         | 5  |
| 765.51       | 1         | r     | Clast-poor sandy diamicite (7)                                       | 756.19           | 774.94            | 17.7      | 19                           | 16     | 11  | 1   | 5   | 48          |        | 13 | x   | x   | x                       | 12 |
| 767.59       | 8         | s-r   | Clast-poor sandy diamicite (7)                                       | 756.19           | 774.94            | 17.8      | 19                           | 16     | 11  | 1   | 5   | 48          |        | 13 | x   | x   | x                       | 12 |
| 866.79       | 2         | s-a   | Sandy mudstone (siltstone) with dispersed clasts (2)                 | 846.06           | 872.70            |           | 2                            | 8      | 1   |     | 2   | 87          |        | 1  | x   | x   | x                       | 7  |
| 965.26       | 3         | r     | Sandy conglomerate (9)   | 964.86           | 965.43            | >19.8     | 8                            | 21     | 2   |     | 1   | 68          |        | 15 | x   | x   | x                       | 5  |
| 996.65       | 3         | r     | Clast-poor sandy diamicite, black (7)                                | 981.01           | 996.69            |           |                              | 2      | 1   | 1   | 1   | 95          |        | 8  | x   | x   | x                       | 9  |
| 1048.38      | 2         | s-r   | Clast-poor sandy diamicite (7)                                       | 1044.06          | 1064.47           |           | 3                            | 9      | 1   | 1   | 1   | 85          |        | 7  | x   | x   |                         | 2  |
| 1075.20      | 6         | s-a   | Clast-poor sandy diamicite (7)                                       | 1065.91          | 1076.15           |           | 2                            | 11     | 2   |     |     | 85          |        | 11 | x   | x   | x                       | 14 |
| 1122.22      | 5         | r     | Clast-poor sandy diamicite (7)                                       | 1109.47          | 1124.93           | <20.25    | 6                            | 12     | 6   | 1   |     | 71          | 4      | 9  | x   | x   | x                       | 5  |

Note: Clast composition after Sandroni and Talarico (2011). Lithofacies and clast dimension and shape after Fielding et al. (2008–09). \*Lithofacies numbers as defined by Fielding et al. (2008–2009). Age after Acton et al. (2008–2009) with modifications as in ANDRILL South McMurdo Sound Science Team (2010) and Di Vincenzo et al. (2010). Abbreviations: mbsf—meters below sea floor; Met—metamorphic rocks; Intrus—intrusive rocks; Qtz—quartz; Dol—dolomite; Volc—volcanic rocks; Intrac—intraclasts; a—angular; s-a—subangular; s-r—subrounded; r—rounded; RSR—Royal Society Range; SM—Skelton-Mulock glacier area; BR—Britannia Range.

TABLE 2. MINERALOGICAL ASSEMBLAGES OF INVESTIGATED CA-AMPHIBOLE-BEARING METAMORPHIC CLASTS IN AND-2A CORE AND OF REPRESENTATIVE SAMPLES OF CA-AMPHIBOLE-BEARING METAMORPHIC ROCKS FROM OUTCROPS IN THE CRYSTALLINE BASEMENT OF THE ROSS OROGEN IN THE REGION COMPRISED BETWEEN FERRAR AND BYRD GLACIERS

| Sample (mbsf) | Latitude (S) | Longitude (E) | Core (an) | PI Rim (an) | Bt XMg (%) | Cam XMg (%) | Kfs (%) | Qtz (%) | Cpx XMg (%) | Opm (%) | Cal (%) | Ttn (%) | Czo-Ep (%) | Grain size | Lithology     |
|---------------|--------------|---------------|-----------|-------------|------------|-------------|---------|---------|-------------|---------|---------|---------|------------|------------|---------------|
| 169.20        |              |               | (45-79)   | (48-84)     | 0          | 0.65        | 0.00    | ●       | ●           | ○       | ○       | ○       | ○          | vfg-fg     | Metasandstone |
| 177.68        |              |               | (30-62)   | (24-26)     | ●          | 0.37        | 0.03    | ●       | ●           | ○       | ○       | ○       | ○          | vfg        | Metasandstone |
| 185.36        |              |               | (23-27)   | (74-79)     | ●          | 0.37        | 0.03    | ●       | ●           | ○       | ○       | ○       | ○          | mg         | Gneiss        |
| 243.16        |              |               | (77-82)   | (28-32)     | ●          | 0.56        | 0.01    | ●       | ●           | ○       | ○       | ○       | ○          | fg-mg      | Cam schist    |
| 285.28        |              |               | (25-33)   | (61-74)     | ●          | 0.68        | 0.02    | ●       | ●           | ○       | ○       | ○       | ○          | fg-mg      | Gneiss        |
| 328.27        |              |               | (62-64)   | (27-29)     | ●          | 0.55        | 0.01    | ●       | ●           | ○       | ○       | ○       | ○          | vfg+fg     | Schist        |
| 352.93        |              |               | (28-31)   | (29-30)     | ●          | 0.52        | 0.01    | ●       | ●           | ○       | ○       | ○       | ○          | fg         | Bt-Cam schist |
| 579.42        |              |               | (43-89)   | (45-81)     | ○          | 0.66        | 0.01    | ●       | ●           | ○       | ○       | ○       | ○          | fg         | Gneiss        |
| 622.68        |              |               | (63-84)   | (78-83)     | ○          | 0.66        | 0.01    | ●       | ●           | ○       | ○       | ○       | ○          | vfg-fg     | Metasandstone |
| 692.00        |              |               | (38-43)   | (39-53)     | ○          | 0.76        | 0.00    | ●       | ●           | ○       | ○       | ○       | ○          | vfg-fg     | Cam-Bt schist |
| 698.67        |              |               | (39-40)   | (24-34)     | ○          | 0.62        | 0.01    | ●       | ●           | ○       | ○       | ○       | ○          | mg         | Ca-silicate   |
| 765.51        |              |               | (67-72)   | (55-65)     | ○          | 0.67        | 0.03    | ●       | ●           | ○       | ○       | ○       | ○          | mg         | granofels     |
| 767.58        |              |               | (52)      | (35-45)     | ○          | 0.59        | 0.06    | ●       | ●           | ○       | ○       | ○       | ○          | mg         | Orthogneiss   |
| 866.79        |              |               | (85-95)   | (79-98)     | ○          | 0.66        | 0.02    | ●       | ●           | ○       | ○       | ○       | ○          | fg         | Orthogneiss   |
| 965.26        |              |               | (42-46)   | (41-51)     | ○          | 0.67        | 0.04    | ●       | ●           | ○       | ○       | ○       | ○          | mg         | Cam-Bt schist |
| 996.65        |              |               | (39-65)   | (37-40)     | ○          | 0.64        | 0.02    | ●       | ●           | ○       | ○       | ○       | ○          | fg         | Metasandstone |
| 1048.38       |              |               | (50-66)   | (53-64)     | ○          | 0.67        | 0.06    | ●       | ●           | ○       | ○       | ○       | ○          | fg         | Amphibolite   |
| 1075.20       |              |               |           |             | ○          | 0.64        | 0.02    | ●       | ●           | ○       | ○       | ○       | ○          | fg-mg      | Bt-Cam schist |
| 1122.22       |              |               |           |             | ○          | 0.67        | 0.06    | ●       | ●           | ○       | ○       | ○       | ○          | fg         | Bt-Cam schist |
|               |              |               |           |             | ○          | 0.67        | 0.03    | ●       | ●           | ○       | ○       | ○       | ○          | fg         | Schist        |

| Sample (outcrops) | Latitude (S) | Longitude (E) | Core (an) | PI Rim (an) | Bt XMg (%) | Cam XMg (%) | Kfs (%) | Qtz (%) | Cpx XMg (%) | Opm (%) | Grt (%) | Ttn (%) | Czo-Ep (%) | Grain size | Lithology         |
|-------------------|--------------|---------------|-----------|-------------|------------|-------------|---------|---------|-------------|---------|---------|---------|------------|------------|-------------------|
| 18-12-03F22B      | 77°52'49"    | 163°55'37"    | (63)      | (62)        | ○          | 0.64        | 0.00    | ●       | ●           | ○       | ○       | ○       | ○          | vfg-fg     | Cam-Bt schist     |
| 23-12-03RF27B     | 78°03'18"    | 164°11'38"    | (76)      | (77)        | ○          | 0.65        | 0.00    | ●       | ●           | ○       | ○       | ○       | ○          | fg-mg      | Amphibolite       |
| 18-12-03F7        | 78°11'01"    | 162°44'18"    |           |             | ○          | 0.65        | 0.00    | ●       | ●           | ○       | ○       | ○       | ○          | fg-mg      | Schist            |
| 23-12-03RRF18     | 78°08'01"    | 163°56'30"    |           |             | ○          |             |         | ●       | ●           | ○       | ○       | ○       | ○          | fg-mg      | Ca-silicate       |
| 21-01-06T2        | 79°02'52"    | 161°53'04"    | (54)      | (41)        | ○          | 0.68        | 0.00    | ●       | ●           | ○       | ○       | ○       | ○          | vfg-fg     | granofels         |
| 17-12-03FR13      | 78°49'50"    | 162°26'06"    | (40)      | (40)        | ○          | 0.58        | 0.00    | ●       | ●           | ○       | ○       | ○       | ○          | vfg        | Metasandstone     |
| 12-12-00T4        | 80°11'58"    | 159°13'00"    | (45-46)   | (46-47)     | ○          | 0.47        | 0.00    | ●       | ●           | ○       | ○       | ○       | ○          | mg-cg      | Phyllite          |
| 19-01-06T2        | 80°23'14"    | 157°09'50"    | (82-82)   | (82-83)     | ○          | 0.49        | 0.03    | ●       | ●           | ○       | ○       | ○       | ○          | fg-mg      | Gneiss            |
| 20-01-06T1        | 79°55'24"    | 158°20'42"    | (37-44)   | (36-43)     | ○          | 0.40        | 0.00    | ●       | ●           | ○       | ○       | ○       | ○          | mg-cg      | Gneiss            |
| 20-01-06T2        | 79°55'24"    | 158°20'42"    | (37-44)   | (39-42)     | ○          | 0.32        | 0.01    | ●       | ●           | ○       | ○       | ○       | ○          | mg-cg      | Metagranodiorite  |
|                   |              |               |           |             | ○          | 0.32        | 0.01    | ●       | ●           | ○       | ○       | ○       | ○          | mg-cg      | meta-granodiorite |

○ = 0 ± 1%    ⊙ = 2 ± 15%    ● = 16 ± 40%    ●>40%

Note: Mineral abbreviations according to Kretz (1983), with the addition of Opm to indicate opaque minerals. Other abbreviations: mbsf—meters below sea floor; XMg—Mg/(Mg+Fe2+); vfg—very fine grained; fg—fine-grained; mg—medium-grained; cg—coarse-grained.

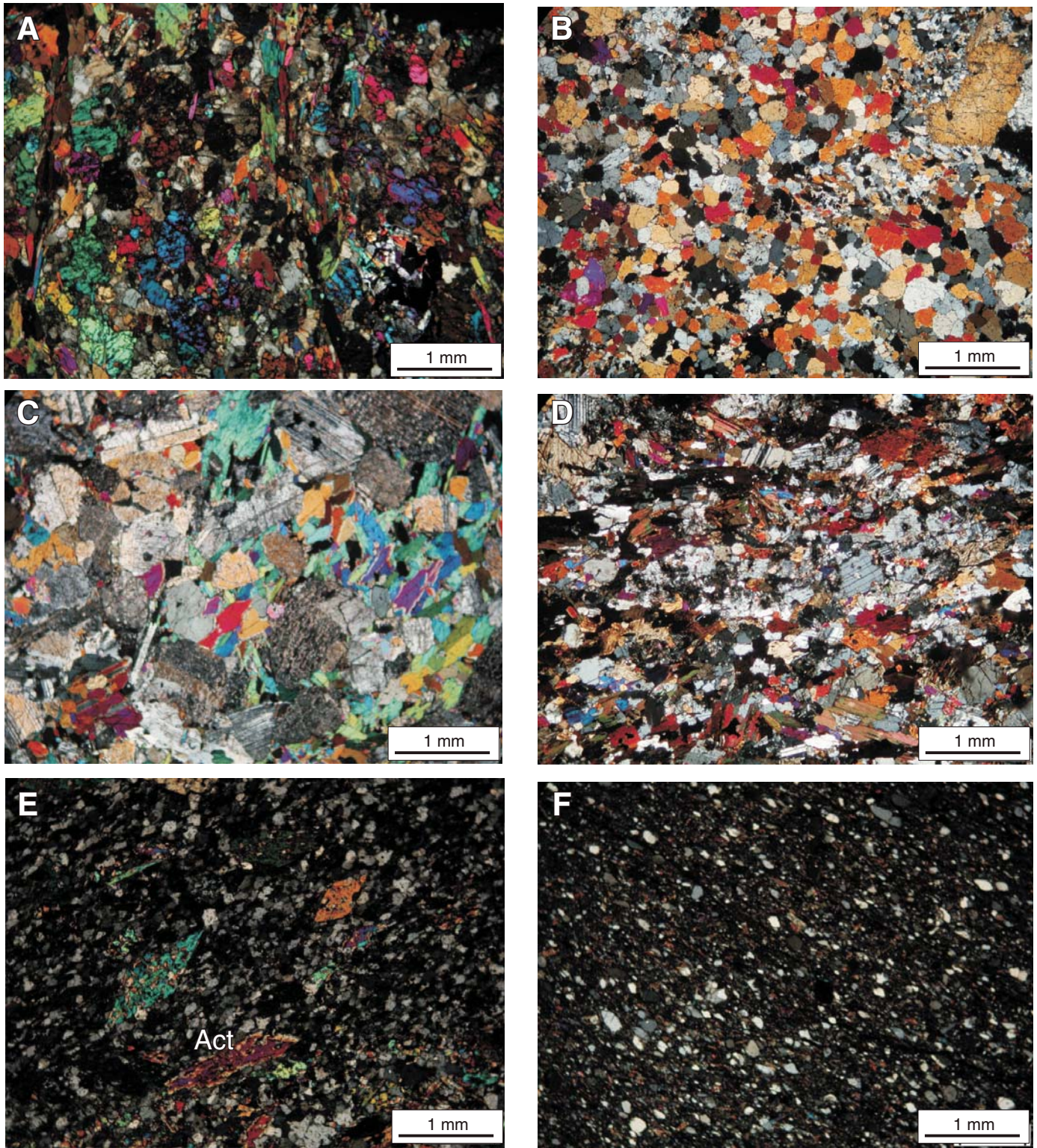
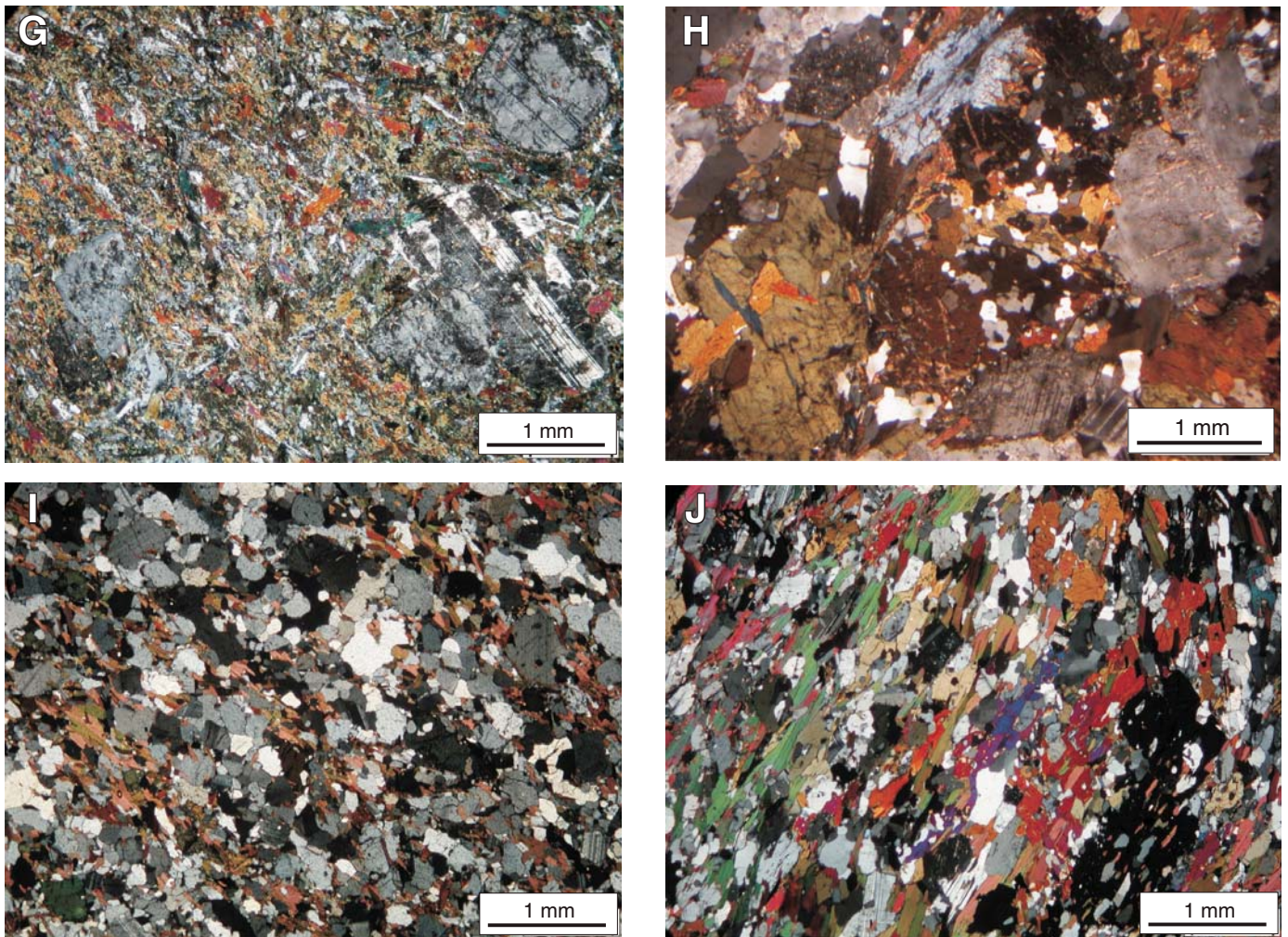


Figure 3 (continued on following page). Microphotographs of the most representative Ca-amphibole-bearing metamorphic clasts (left column) and of petrographically similar lithologies (right column) from the potential source rock units in the basement exposed in the region between Ferrar and Byrd glaciers (see Fig. 1 for their location) (all taken with crossed polarizers). (A) and (B) Ca-amphibole-bearing diopside-plagioclase granofels: (A) clast 698.67 mbsf, (B) sample 23-12-03RF18 (Miers Valley, Royal Society Range); (C) and (D) amphibolite: (C) clast 996.65 mbsf, (D) sample 23-12-03RF27B (Garwood Valley, Royal Society Range); (E) and (F) Ca-amphibole-bearing metasandstone: (E) clast 622.68 mbsf (with randomly oriented poikiloblasts of actinolite [Act]), (F) sample 21-01-06T2 (Teall Island, Skelton Glacier).



**Figure 3 (continued).** (G) and (H) Ca-amphibole-bearing orthogneiss: (G) clast 767.58 mbsf, (H) sample 20-01-06T1 (Darwin Glacier, Britannia Range); (I) and (J) Ca-amphibole-bearing paragneiss: (I) clast 579.42 mbsf, (J) sample 19-01-06T2 (Byrd Glacier, Britannia Range).

the AND-2A core (Zattin et al., 2010; Sandroni and Talarico, 2011), provided evidence of a number of diagnostic lithologies that closely match the lithological variability of the crystalline basement in South Victoria Land and strongly support a provenance from the region between the present-day Blue-Koettlitz and Mulock glaciers (Fig. 1).

The mineralogical and microstructural features of investigated AND-2A Ca-amphibole-bearing metamorphic clasts generally show significant similarities with compositionally comparable lithologies from outcrops located in the main exposure areas of the South Victoria Land basement. Table 2 includes ten samples that are part of a collection of over 600 samples collected from 65 localities and that are representative of three regions with partly different metamorphic and lithological features (Royal Society Range, Skelton-Mulock glacier area, and Britannia Range; Fig. 1). The close miner-

alogical similarities are generally accompanied by striking microstructural (Fig. 3) and compositional analogies as indicated by the good fit of most Ca-amphibole compositions in the clasts (including the commonly present slight intracrystalline zoning; see the Supplemental Table [see footnote 1]) within the compositional fields defined by representative samples from the outcrops (Fig. 4).

In Britannia Range samples (and in petrographically similar clasts from the AND-2A core), Ca-amphibole displays sometimes a slight zonation with pargasite, tschermakite, or Mg-hornblende in cores and Fe-tschermakite or Fe-pargasite in rims. In contrast, samples from the Royal Society Range and those from the adjacent Skelton-Mulock glacier area (and the petrographically similar AND-2A clasts) show weak zonations with Mg-hornblende in cores and Mg-hornblende with lower  $^{IV}Al$  or actinolite or tremolite in rims.

The composition of amphibole coexisting with plagioclase (Table 3 and the Supplemental Table [see footnote 1]) is a good tool to semi-quantitatively estimate P-T conditions attending the formation of these mineral assemblages. Actually, Si, Al, and Na distribution in amphibole structural sites depends on physical conditions during crystallization. While  $Si^{4+}$  decreases, Ti,  $^{VI}Al$ , and  $Na^A$  increase with temperature (T), and  $^{IV}Al$  and  $Na^B$  rise with pressure (P) (Raase, 1974; Brown, 1977; Holland and Richardson, 1979; Spear, 1980). The Ca-amphiboles in our samples can be compared with those reported by Zenk and Schulz (2004), who provided detailed microstructural, mineral chemical, and thermobarometric data on Ca-amphibole-bearing assemblages from the classical Barrovian metamorphic zones in the Dalradian Group in Scotland. As in the Dalradian Group, our samples similarly show the coexistence of Ca-amphiboles with



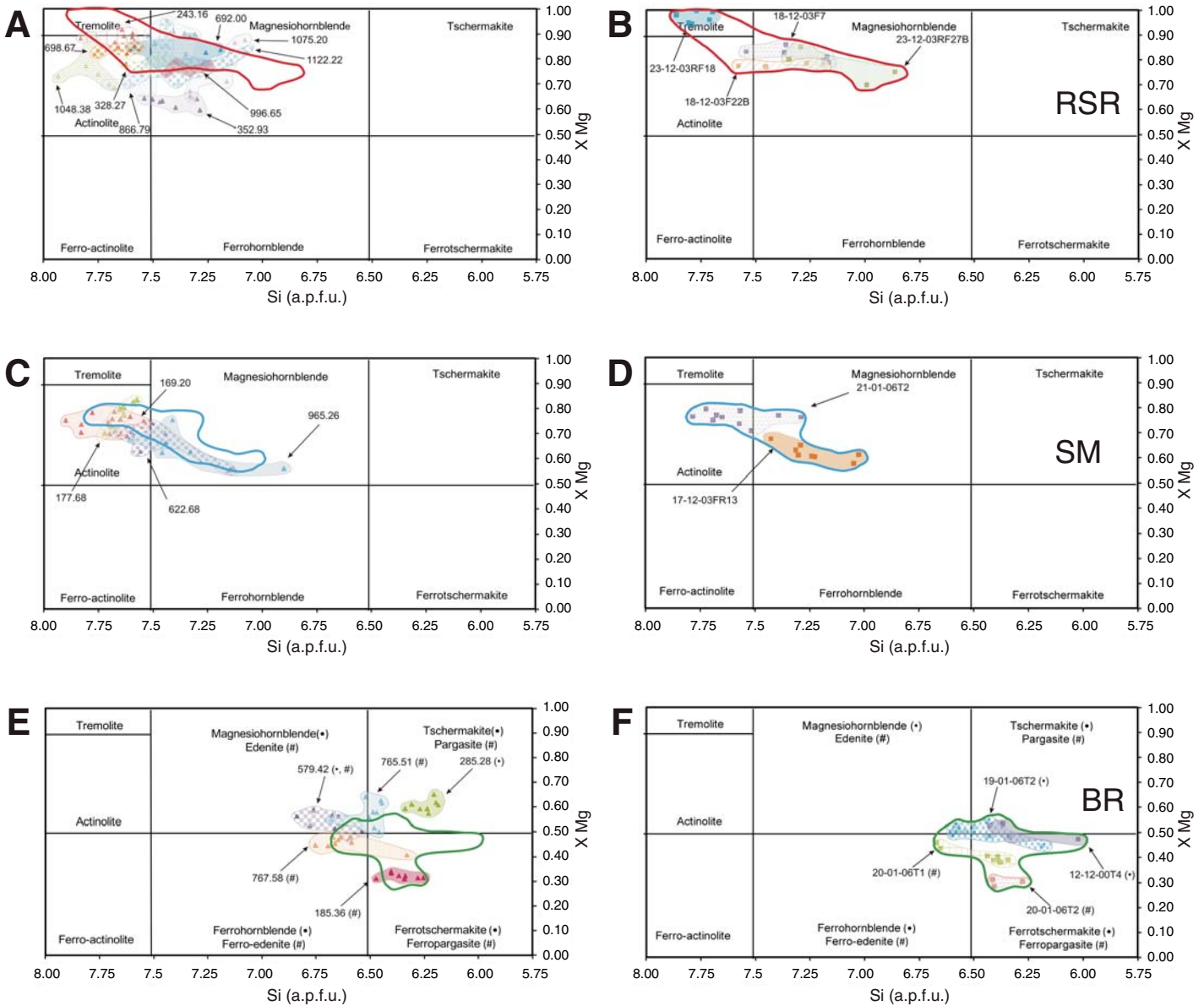


**Figure 4.** Compositional diagrams showing the compositional variability of Ca-amphibole in AND-2A clast samples (A, C, and E) and their similarity with samples from potential rock units in the Royal Society Range (B), Mulock-Skelton glacier area (D), and Britannia Range (F) (nomenclature after Leake et al., 1997). Symbols in (E) and (F) (•, #) refer to Ca-amphiboles characterized by  $(\text{Na}+\text{K})_{\text{A}} < 0.50$ ;  $\text{Ti} < 0.50$ , and  $(\text{Na}+\text{K})_{\text{A}} \geq 0.50$ ;  $\text{Ca}_{\text{A}} < 0.50$  parameters, respectively.  $\text{XMg} = \text{Mg}/(\text{Mg} + \text{Fe}^{2+})$ ; a.p.f.u. = atoms per formula unit.

plagioclases ranging in composition from oligoclase (typical of the biotite zone) to, more frequently, andesine and/or labradorite (garnet or kyanite zone).

Results of the application of the empirical Ca-amphibole geothermobarometry using the analytical expression given by Zenk and Schulz (2004) and Gerya et al. (1997) are listed in Table 3 and shown in Figure 5. The two methods gave similar T results, whereas P values calculated with Zenk and Schulz's (2004) geobarometer are 1–1.5 kb higher

than those obtained using the Gerya et al. (1997) barometer.

In most samples the variation ranges of estimated P-T values are within the absolute error ranges ( $\pm 1.2$  kb and  $\pm 37$  °C) of both geothermobarometric methods. However, all samples show a certain variability of P-T values with systematic trends reflecting intracrystalline compositional variations of Ca-amphibole grains according, as described above, to two distinct zoning patterns. In samples from the Britannia Range and petrographically similar clasts,

the highest P and T values (up to 7–8 kb, 660 °C) were obtained using the composition of Fe-tschermakite rims, whereas the minimum values (4.1–5.5 kb and 560–595 °C) are due to Mg-hornblende or edenite/Fe-edenite compositions preserved in core grains. In all other clasts and samples from outcrops (i.e., those from the Royal Society Range and Mulock-Skelton glacier area), maximum P and T values are given by core compositions, whereas rim compositions yield lower P-T values. The overall P-T estimates are significantly lower (~2–4 kb,

TABLE 3. RESULTS OF CA-AMPHIBOLE GEOTHERMOMETRY IN AND-2A METAMORPHIC CLASTS AND SELECTED SAMPLES FROM THE CRYSTALLINE BASEMENT IN THE ROYAL SOCIETY RANGE. THE AREA COMPRISED BETWEEN MULOCK AND SKELTON GLACIERS AND THE BRITANNIA RANGE

|                        |  | Koettlitz-Blue glacier area |        |        |            |        |        |              |        |        |              |        |        |                 |        |        |              |        |        |            |        |  |            |  |  |            |  |  |
|------------------------|--|-----------------------------|--------|--------|------------|--------|--------|--------------|--------|--------|--------------|--------|--------|-----------------|--------|--------|--------------|--------|--------|------------|--------|--|------------|--|--|------------|--|--|
|                        |  | 328.27                      |        |        | 352.93     |        |        | 622.00       |        |        | 698.67       |        |        | 866.79          |        |        | 996.65       |        |        | 1048.38    |        |  | 1075.20    |  |  | 1122.22    |  |  |
|                        |  | 2 core                      | 2 rim  | 1 core | 1 rim      | 1 core | 2 rim  | 1 core       | 1 rim  | 4 core | 4 rim        | 6 core | 6 rim  | 4 core          | 1 rim  | 2 core | 2 rim        | 3 core | 3 rim  | 5 core     | 5 rim  |  |            |  |  |            |  |  |
| Si                     |  | 7.672                       | 7.829  | 7.304  | 7.486      | 7.299  | 7.501  | 7.267        | 7.595  | 7.585  | 7.748        | 7.493  | 7.700  | 7.320           | 7.433  | 7.675  | 7.782        | 7.176  | 7.252  | 7.394      | 7.602  |  |            |  |  |            |  |  |
| Altot                  |  | 0.612                       | 0.343  | 1.121  | 0.770      | 1.081  | 0.795  | 1.111        | 0.597  | 0.652  | 0.408        | 0.649  | 0.443  | 1.039           | 0.903  | 0.581  | 0.298        | 1.196  | 1.170  | 0.872      | 0.872  |  |            |  |  |            |  |  |
| Fe3+                   |  | 0.000                       | 0.014  | 0.163  | 0.033      | 0.163  | 0.081  | 0.426        | 0.464  | 0.115  | 0.000        | 0.605  | 0.041  | 0.123           | 0.011  | 0.000  | 0.566        | 0.167  | 0.269  | 0.154      | 0.039  |  |            |  |  |            |  |  |
| TOTAL                  |  | 15.047                      | 14.926 | 15.076 | 15.107     | 14.984 | 15.041 | 14.856       | 14.791 | 15.132 | 15.131       | 14.975 | 15.108 | 15.245          | 15.240 | 15.178 | 14.855       | 15.357 | 15.138 | 15.237     | 15.083 |  |            |  |  |            |  |  |
| Gerya et al. (1997)    |  |                             |        |        |            |        |        |              |        |        |              |        |        |                 |        |        |              |        |        |            |        |  |            |  |  |            |  |  |
| T (°C)                 |  | 418                         | 380    | 477    | 452        | 471    | 445    | 467          | 409    | 439    | 412          | 441    | 418    | 487             | 470    | 428    | 382          | 514    | 489    | 477        | 432    |  |            |  |  |            |  |  |
| P (kb)                 |  | 1.9                         | 1.3    | 2.9    | 2.3        | 2.8    | 2.3    | 2.9          | 2.0    | 2.1    | 1.6          | 2.3    | 1.7    | 2.9             | 2.6    | 2.0    | 1.5          | 3.3    | 3.1    | 2.6        | 2.4    |  |            |  |  |            |  |  |
| Zenk and Schulz (2004) |  |                             |        |        |            |        |        |              |        |        |              |        |        |                 |        |        |              |        |        |            |        |  |            |  |  |            |  |  |
| T (°C)                 |  | 418                         | 380    | 477    | 452        | 471    | 445    | 467          | 409    | 439    | 412          | 441    | 418    | 487             | 470    | 428    | 382          | 514    | 489    | 477        | 432    |  |            |  |  |            |  |  |
| P (kb)                 |  | 2.0                         | 1.3    | 3.4    | 2.4        | 3.2    | 2.5    | 3.4          | 2.2    | 2.3    | 1.6          | 2.6    | 1.7    | 3.3             | 2.9    | 2.1    | 1.7          | 3.8    | 3.7    | 2.9        | 2.7    |  |            |  |  |            |  |  |
|                        |  | Skelton-Mulock glacier area |        |        |            |        |        |              |        |        |              |        |        | Britannia Range |        |        |              |        |        |            |        |  |            |  |  |            |  |  |
|                        |  | 177.68                      |        |        | 622.68     |        |        | 965.26       |        |        | 185.36       |        |        | 285.28          |        |        | 579.42       |        |        | 765.51     |        |  | 767.58     |  |  |            |  |  |
|                        |  | 8 core                      | 2 rim  | 1      | 3          | 2 core | 2 rim  | 3 core       | 4 rim  | 1 core | 4 rim        | 1 core | 1 rim  | 3 core          | 3 rim  | 3 core | 2 rim        | 2 core | 1 rim  | 2 core     | 1 rim  |  |            |  |  |            |  |  |
| Si                     |  | 7.704                       | 7.899  | 7.693  | 7.632      | 7.145  | 7.560  | 6.901        | 7.436  | 6.474  | 6.256        | 6.309  | 6.238  | 6.838           | 6.540  | 6.447  | 6.683        | 6.695  | 6.663  | 6.695      | 6.663  |  |            |  |  |            |  |  |
| Altot                  |  | 1.547                       | 1.030  | 0.829  | 0.553      | 1.441  | 0.749  | 1.782        | 1.106  | 2.029  | 2.355        | 2.548  | 2.661  | 1.601           | 1.914  | 2.395  | 2.232        | 2.084  | 2.380  | 2.084      | 2.380  |  |            |  |  |            |  |  |
| Fe3+                   |  | 0.000                       | 0.000  | 0.000  | 0.209      | 0.000  | 0.000  | 0.020        | 0.100  | 0.237  | 0.308        | 0.627  | 0.679  | 0.398           | 0.359  | 0.254  | 0.000        | 0.000  | 0.000  | 0.000      | 0.000  |  |            |  |  |            |  |  |
| TOTAL                  |  | 14.820                      | 14.592 | 14.993 | 15.155     | 15.201 | 15.058 | 15.171       | 14.927 | 15.664 | 15.732       | 15.383 | 15.373 | 15.373          | 15.604 | 15.594 | 15.576       | 15.595 | 15.542 | 15.595     | 15.542 |  |            |  |  |            |  |  |
| Gerya et al. (1997)    |  |                             |        |        |            |        |        |              |        |        |              |        |        |                 |        |        |              |        |        |            |        |  |            |  |  |            |  |  |
| T (°C)                 |  | 392                         | 332    | 410    | 433        | 508    | 437    | 540          | 446    | 622    | 651          | 628    | 636    | 560             | 611    | 622    | 591          | 591    | 592    | 591        | 592    |  |            |  |  |            |  |  |
| P (kb)                 |  | 2.9                         | 1.7    | 1.7    | 2.1        | 3.5    | 2.2    | 4.1          | 2.7    | 4.9    | 5.5          | 5.9    | 6.1    | 4.1             | 4.7    | 5.5    | 5.1          | 4.8    | 5.4    | 4.8        | 5.4    |  |            |  |  |            |  |  |
| Zenk and Schulz (2004) |  |                             |        |        |            |        |        |              |        |        |              |        |        |                 |        |        |              |        |        |            |        |  |            |  |  |            |  |  |
| T (°C)                 |  | 392                         | 332    | 410    | 433        | 508    | 437    | 540          | 446    | 622    | 651          | 628    | 636    | 560             | 611    | 622    | 591          | 591    | 592    | 591        | 592    |  |            |  |  |            |  |  |
| P (kb)                 |  | 3.6                         | 2.1    | 1.8    | 2.2        | 4.1    | 2.3    | 4.8          | 3.2    | 5.7    | 6.6          | 7.3    | 7.6    | 4.8             | 5.5    | 6.8    | 6.2          | 5.7    | 6.5    | 5.7        | 6.5    |  |            |  |  |            |  |  |
|                        |  | Koettlitz-Blue glacier area |        |        |            |        |        |              |        |        |              |        |        | Britannia Range |        |        |              |        |        |            |        |  |            |  |  |            |  |  |
|                        |  | 23-12-03RF27B               |        |        | 18-12-03F7 |        |        | 23-12-03RF18 |        |        | 18-12-03F22B |        |        | 21-01-06T2      |        |        | 17-12-03FR13 |        |        | 20-01-06T1 |        |  | 12-12-00T4 |  |  | 19-01-06T2 |  |  |
|                        |  | 2 core                      | 2 rim  | 2 core | 3 rim      | 1 core | 1 rim  | 1 core       | 1 rim  | 5 core | 5 rim        | 1 core | 2 rim  | 2 core          | 2 rim  | 1 core | 2 rim        | 2 core | 2 rim  | 2 core     | 2 rim  |  |            |  |  |            |  |  |
| Si                     |  | 6.863                       | 7.294  | 7.166  | 7.362      | 7.711  | 7.862  | 7.191        | 7.580  | 7.288  | 7.785        | 7.026  | 7.427  | 6.406           | 6.278  | 6.654  | 6.344        | 6.338  | 6.023  | 6.441      | 6.187  |  |            |  |  |            |  |  |
| Altot                  |  | 1.562                       | 0.914  | 1.139  | 0.795      | 0.249  | 0.129  | 1.192        | 0.707  | 1.015  | 0.445        | 1.339  | 0.828  | 2.317           | 2.460  | 1.958  | 2.412        | 2.556  | 3.208  | 2.153      | 2.914  |  |            |  |  |            |  |  |
| Fe3+                   |  | 0.459                       | 0.657  | 0.506  | 0.600      | 0.214  | 0.141  | 0.301        | 0.097  | 0.191  | 0.000        | 0.168  | 0.193  | 0.000           | 0.093  | 0.137  | 0.159        | 0.343  | 0.576  | 0.532      | 0.251  |  |            |  |  |            |  |  |
| TOTAL                  |  | 15.159                      | 14.980 | 15.209 | 15.062     | 15.224 | 15.068 | 15.230       | 15.096 | 15.270 | 15.084       | 15.456 | 15.249 | 15.639          | 15.749 | 15.552 | 15.668       | 15.395 | 15.336 | 15.370     | 15.479 |  |            |  |  |            |  |  |
| Gerya et al. (1997)    |  |                             |        |        |            |        |        |              |        |        |              |        |        |                 |        |        |              |        |        |            |        |  |            |  |  |            |  |  |
| T (°C)                 |  | 544                         | 472    | 506    | 467        | 426    | 387    | 504          | 437    | 493    | 402          | 541    | 471    | 629             | 649    | 594    | 638          | 625    | 660    | 611        | 647    |  |            |  |  |            |  |  |
| P (kb)                 |  | 3.9                         | 2.8    | 3.3    | 2.6        | 1.6    | 1.2    | 3.3          | 2.2    | 2.9    | 1.7          | 3.6    | 2.6    | 5.2             | 5.6    | 4.7    | 5.5          | 5.7    | 7.0    | 5.1        | 6.4    |  |            |  |  |            |  |  |
| Zenk and Schulz (2004) |  |                             |        |        |            |        |        |              |        |        |              |        |        |                 |        |        |              |        |        |            |        |  |            |  |  |            |  |  |
| T (°C)                 |  | 544                         | 472    | 506    | 467        | 426    | 387    | 504          | 437    | 493    | 402          | 541    | 471    | 629             | 649    | 594    | 638          | 625    | 660    | 611        | 647    |  |            |  |  |            |  |  |
| P (kb)                 |  | 4.6                         | 3.3    | 3.8    | 3.0        | 1.5    | 1.0    | 3.8          | 2.4    | 3.3    | 1.7          | 4.1    | 2.9    | 6.2             | 6.7    | 5.5    | 6.6          | 7.1    | 8.8    | 6.2        | 7.9    |  |            |  |  |            |  |  |

Note: Pressure (P)-temperature (T) estimates are based on the empirical Ca-amphibole geothermometry after Zenk and Schulz (2004) and Gerya et al. (1997). Ca-amphibole compositional parameters (Si, Al, Fe3+) used in the calculations are number of cations normalized to 23 oxygens and sum (T1 + T2 + M1 + M2 + M3) = 13 as detailed by Triboulet (1992), with Fe3+ estimated as maximum according to Paplike et al. (1974). Error ranges: T (±37 °C), P (±1.2 kb).

~400–600 °C) than those estimated for the Britannia Range samples. In contrast, samples from the Royal Society Range and those from the adjacent Skelton-Mulock glacier area show perfectly overlapping P-T results. Nevertheless, published P-T estimates (Talarico et al., 2005; Cook and Craw, 2001, 2002) and the distinctly different fabrics of the samples from the two regions indicate significantly different initial regional metamorphic conditions and variably developed contact-metamorphic effects (Fig. 6A). In the Skelton-Mulock glacier area, investigated

metasandstones show general petrographic features consistent with a low-grade regional metamorphic peak, but the microstructural features of Ca-amphibole (occurring as randomly oriented poikiloblasts) indicate its post-tectonic growth likely as the result of contact metamorphism under higher T conditions. According to the Ca-amphibole geothermobarometry, this contact-metamorphic event would have occurred at P < 4 kb. Similar values are reported by Wynyard (2004) as emplacement depth of post-tectonic granitoids in the region.

In the Royal Society Range, the metamorphic pattern includes a wide region of high-grade conditions with more restricted areas of medium to low grade confined to the area including the upper Walcott and Radian glaciers (Fig. 6A). As indicated by the investigated samples, the high-grade region also suffered lower-grade reequilibration and, as commonly observed in similar metamorphic terrains (Vernon, 1976; Miyashiro, 1994; Bucker and Frey, 1994; Vernon and Clarke, 2008), the low-grade overprint may be often complete enough to erase early high-grade

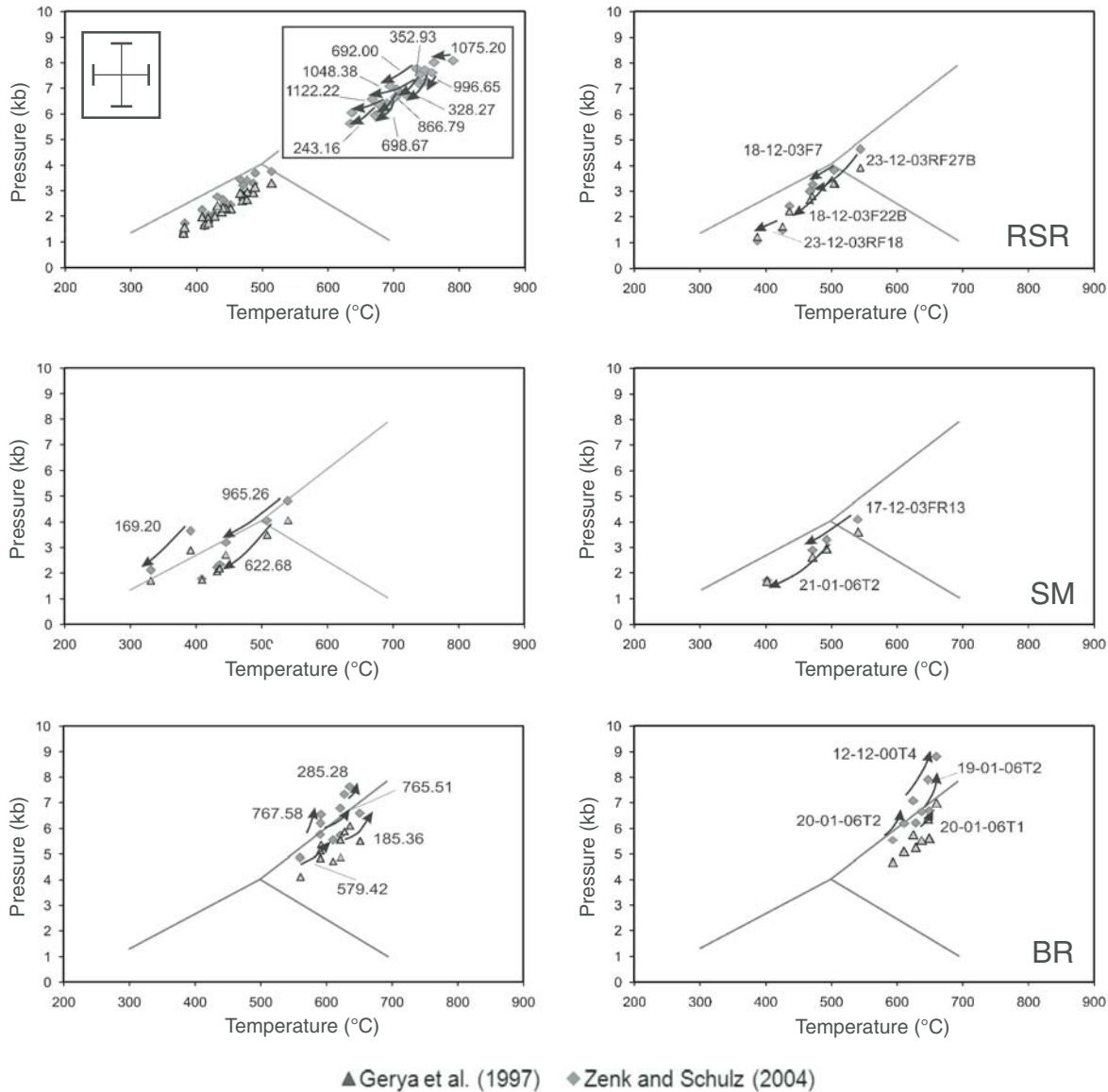


Figure 5. Pressure-temperature (P-T) data and P-T paths from Ca-amphibole mineral assemblages in AND-2A metamorphic clasts (left) and representative samples from their most likely provenance regions (right). RSR—Royal Society Range; SM—Skelton-Mulock glacier area; BR—Britannia Range. Thermobarometric data are affected by minimum error of 38 °C/1.2 kb. Arrows indicate P-T evolution trends according to amphibole core-to-rim zonations (the arrow head indicates rim compositions).  $Al_2SiO_5$  phase boundaries in broken lines according to Spear (1993).

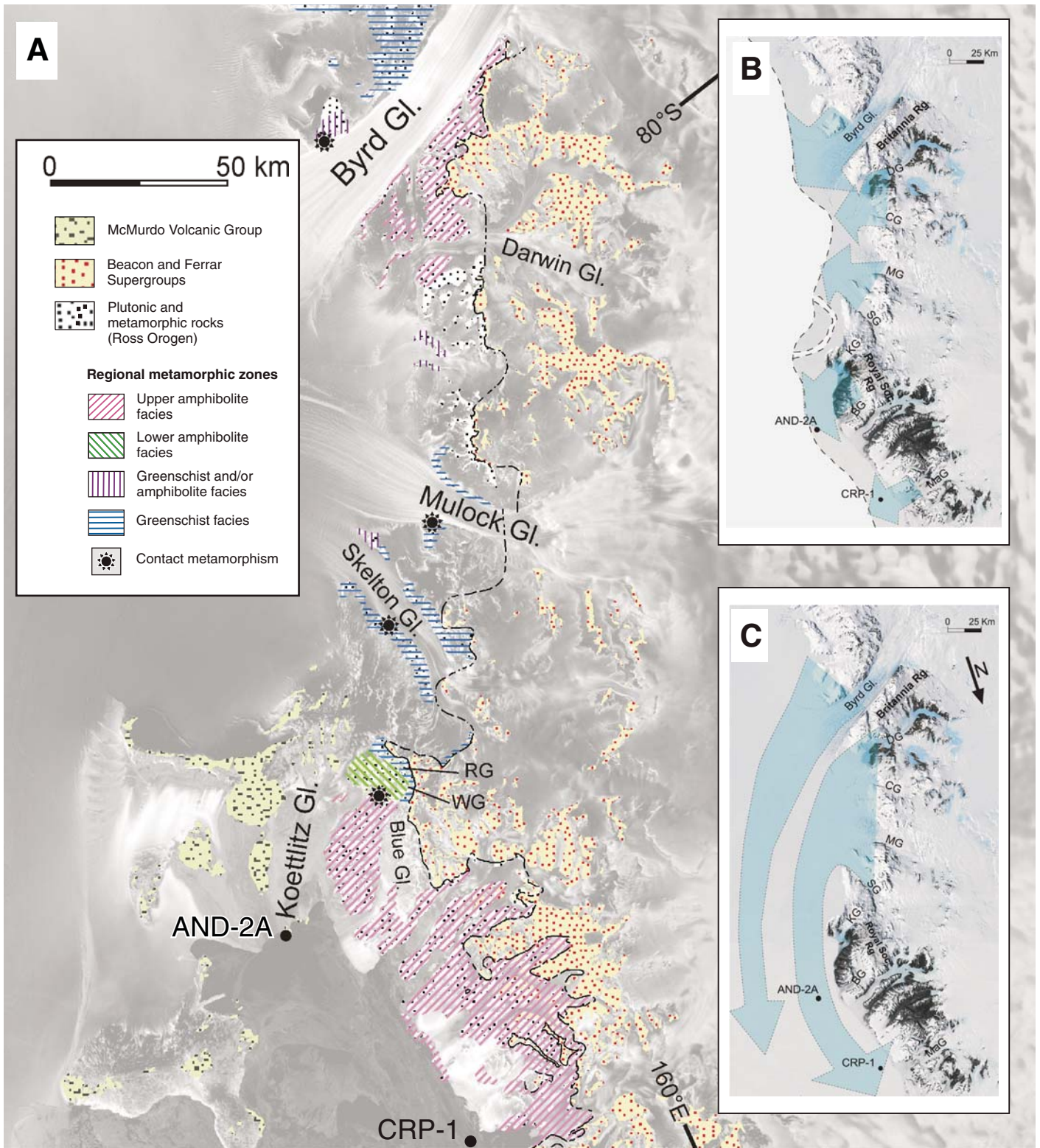


Figure 6. (A) Metamorphic pattern of the Ross Orogen in South Victoria Land. The map is based on the results of petrological investigations reported in Talarico et al. (2007) (Byrd Glacier area); Carosi et al. (2007) (Britannia Range); Cottle (2002) (Carlyon Glacier area); Cook and Craw (2002), Wynyard (2004) (Skelton-Mulock glacier area); Cook and Craw (2001), Talarico et al. (2005), Findlay et al. (1984) (Royal Society Range); Allibone (1992), Cox (1992) (Ferrar-Mackay glacier area). (B) and (C) show two schematic glacial scenarios for the supply of debris to the AND-2A drill site from the different provenance regions indicated by the clast petrology in the AND-2A core sections below 650 mbsf. The present-day paleogeography has been modified by omitting volcanic centers with age <17 Ma. Gl.—Glacier.

paragenesis and/or mineral compositions from the rock metamorphic record. Advanced to complete low-grade reequilibrations are generally more common in highly deformed rock volumes (i.e., from shear zones) and in pelitic and/or semipelitic bulk rock compositions. Such compositions are typical of most of the investigated clast samples.

## INTERPRETATIONS AND DISCUSSION

The results of petrological investigations on Ca-amphibole-bearing metamorphic clasts provide evidence of three distinct provenance regions for the supply of these basement clasts to the AND-2A drill site area. All three regions are located in the Transantarctic Mountains segment comprised between Ferrar and Byrd glaciers, and include from N to S and at increasing distance from the AND-2A drill site: the Royal Society Range, the Skelton-Mulock glacier area, and the Britannia Range (Figs. 1 and 6A). Although the study demonstrates the value of the mineralogical features of the investigated clast assemblage as a useful provenance tool, a deeper analysis and discussion of the results need the consideration of a number of additional constraints reflecting the observed variability in terms of clast shapes, host sedimentary lithofacies, overall clast compositions, and distribution in the host lithological unit (i.e., position at the base or top; Table 1). In the following sections, each clast group indicating the three distinct provenances will therefore be discussed taking into account these various aspects with consequent implications for the depositional settings and processes and for glacial reconstructions based on the AND-2A core record.

### The Royal Society Range Provenance

Among the ten analyzed clast samples showing a Royal Society Range provenance signature, most are subrounded to well rounded and occur in several stratified diamictite (lithofacies 7) intervals, 6–24 m thick, either near the base (e.g., 1048.30 mbsf) or more often in the uppermost part. Angular or subangular clasts mainly occur as limestones in fine-grained and clast-poor lithofacies (e.g., lithofacies 5 and 2).

Down-core distribution of clast samples highlights a main concentration of these clasts below 1000 mbsf and, consistent with preliminary provenance inferences (Panter et al., 2008–2009), indicate a well-documented time window (between 20.2 and 20.1 Ma, Acton et al., 2008–2009 with modification as in ANDRILL SMS Science Team, 2010) with ice mainly sourced from the Royal Society Range.

Correlative strata in CRP-1 (Florindo et al., 2005) include diamictites that are devoid of volcanic clasts and carry basement clast lithologies mirroring the local lithological range of the Mackay Glacier area (Talarico and Sandroni, 1998). From this perspective, the regional evidence of local-ice lobes flowing from W to E (Fig. 6B), rather than with flow lines running N-S close to the Transantarctic Mountains front, would be more consistent with fluctuations of East Antarctic Ice Sheet local outlet glaciers than with the presence of an ice sheet covering the entire Ross Embayment. Given its apparent timing, the AND-2A core section with a Royal Society Range provenance (~1050 mbsf to the hole bottom;  $20.1\text{--}20.2 \pm 0.15$  Ma as maximum; Acton et al., 2008–2009, with modifications reported by ANDRILL SMS Science Team, 2010; Di Vincenzo et al., 2010) may record the latter stages of the M11a glaciation (Miller et al., 1996).

### The Skelton-Mulock Glacier Provenance and Britannia Range Provenance

Analyzed samples indicative of provenances from the Skelton-Mulock glacier area and Britannia Range are scattered throughout the AND-2A core. Occurrences in the uppermost 225 m are represented by subrounded to well-rounded clasts that occur near the top of 2- to 10-m-thick massive or stratified diamictites. Based on their petrological affinity, the investigated clasts could indicate the deposition from ice sourced in the present-day region comprised between Skelton and Byrd glaciers. However a number of independent lines suggest that they are most likely reworked debris. First, they represent a very rare occurrence and are mixed with other more abundant basement clasts including several varieties of granitoids, which, based on petrographical data reported in Panter et al. (2008–2009) and in Zattin et al. (2010), closely match the lithological variability of the Royal Society Range. Second, high concentrations of intraclasts occur closely associated to the analyzed clast samples (within the 1- to 0.1-m-long host core sections). Third, the intraclasts commonly include clasts of diamictites with abundant volcanic lithics and small pebbles of metasandstones of a likely Skelton Glacier provenance (Panter et al., 2008–2009). The combination of these various features corroborates the conclusion that provenance signatures deduced for the three clasts above 225 mbsf cannot provide valuable constraints to glacial reconstructions.

Due to the poorly constrained model age, the AND-2A core section above 225 mbsf can only be very approximately compared to other previous drill cores in the McMurdo Sound region.

Potentially correlative diamictites in AND-1B core indicate a provenance from the Skelton-Mulock glacier area (Talarico et al., 2011), leaving the possibility for ice sourced from the Royal Society Range during glacial maxima in the regional glacial scenario.

In contrast, the well-dated core section (below 225 mbsf; 20.2–14.2 Ma; Acton et al., 2008–2009, with modifications reported by the ANDRILL SMS Science Team, 2010; Di Vincenzo et al., 2010) offers a better opportunity to provide constraints to glacial scenarios. Investigated clasts in this core section comprise six samples, with variable shape and size (Table 1). Skelton Glacier-sourced clasts, represented by angular limestones hosted in sandstone (at 622.68 mbsf), can be interpreted as iceberg-rafted debris (IRD). The occurrence of pebbles of volcanic lavas in the same short (10 cm) core interval indicates that major calving processes should have been active mainly in the proto-Mount Morning area (or other volcanic centers underneath the Ross Ice Shelf), where both metamorphic and volcanic bedrock could have been potentially present at the time indicated by recovered sediments. The rounded cobble in thin conglomerate at 965.26 mbsf shows a similar association with abundant volcanics. In this case, the sedimentological interpretation of this lithofacies, indicating ice-proximal environments in the presence of meltwater (Fielding et al., 2008–2009), is consistent with reworking of pristine diamictites with Skelton Glacier-sourced debris that are documented in the underlying core interval (at ~975–995 mbsf).

The Britannia Range-sourced clasts occur as either angular and/or subangular small pebbles at the base of thin (1.5–4 m) stratified diamictites, or as subrounded to rounded pebbles in a 19-m-thick unit of massive diamictites. The occurrence of angular clasts at the base of a diamictite unit is consistent with glacial processes occurring in more ice-distal locations, beyond the maximum extent of glacier advance as described by Fielding et al. (2008–2009). The association with volcanic pebbles and metamorphic rocks indicating mixed (Skelton Glacier and Royal Society Range) provenance requires a complex evolution in order to have the observed final clast composition at the initial phase of deposition. Moreover, similarly to the core section above 225 mbsf, core sections hosting the two occurrences show mixed debris indicating both Skelton-Mulock glacier source and local sources (i.e., Royal Society Range and volcanic centers in the McMurdo Sound). Consequently, the meaning of the two Britannia Range occurrences remains obscure. The very

small thickness of the hosting diamictites (1.5–4 m) appears to be more consistent with IRD than distal deposition related to a massive ice sheet sourced from areas as distant as the Britannia Range. If mixed assemblages could be explained as for the core section above 225 mbsf (i.e., primary Royal Society Range glacial activity and reworking of Skelton Glacier or Britannia Range debris), the preservation of angular shapes would indicate that some clasts could have escaped extensive abrasion during reworking.

In contrast, the two subrounded to rounded pebbles and the overall clast compositional features in the thick unit of massive diamictites at 756–775 mbsf can be explained in terms of a regional-scale ice-flow pattern reflecting a most likely thicker ice sourced from Transantarctic Mountains outlet glaciers between Mulock and Byrd glaciers and with flow lines mainly N-S aligned parallel to the Transantarctic Mountains front (Fig. 6C). This diamictite unit is part of a thick diamictite-dominated core section between 637 and 778 mbsf that consistently shows the same clast composition and dominant Skelton-Mulock glacier area provenance. Actually the two investigated clasts constitute a minor and nonpersistent component of the basement clast assemblages comprising granitoids and metamorphic rocks that are similar to the rock units exposed in the Skelton-Mulock glacier area (Zattin et al., 2010; Sandroni and Talarico, 2011). This core interval shows a prominent hiatus (ca. 1 Ma) at its base (Acton et al., 2008–2009, with modifications reported by ANDRILL SMS Science Team, 2010), and, as interpreted by Passchier et al. (2010), it would represent glacially-dominated depositional environments with periods of grounded ice, major ice growth to volumes larger than the present day, and only brief intervals of ice-free coasts. Interestingly, correlative diamictite sections in CRP-1 (Florindo et al., 2005) show a significant amount of volcanic clasts (Smellie, 1998) most likely sourced from the Mount Morning (Martin et al., 2010), and clay fraction with peaks in smectite concentration that were interpreted by Ehrmann et al. (2005) as indicating the same southern provenance. In this context, the ice-flow pattern can be confidently traced at a regional scale over the entire McMurdo Sound (including AND-2A and CRP-1 drill sites) with flow lines running very close and parallel to the Transantarctic Mountains front (Fig. 6C). In light of the model age (ca. 17.8 Ma at 778 mbsf and ca. 17.3 ± 0.14 Ma at 626 mbsf; Acton et al., 2008–2009, with modifications reported by the ANDRILL SMS Science Team, 2010; Di Vincenzo et al., 2010), it is possible that this core section preserves evidence of the MiB

glaciation (Miller et al., 1996) and a prominent decrease (up to 20 m) of the sea level (Kominz et al., 2008).

## CONCLUSIONS

(1) The gravel fraction in the AND-2A core contains a small group of Ca-amphibole-bearing metamorphic small pebbles and cobbles (angular to well rounded in shape and occurring in different lithofacies) that are scattered throughout the early Miocene to Pliocene section. This clast lithology shows a rather wide range of Ca-amphibole compositions, type of Ca-amphibole intracrystalline zoning, mineral assemblages and fabrics reflecting different bulk rocks and metamorphic conditions. The clasts have been compared with petrographically similar rock types from potential source areas in the crystalline basement exposed in the region between Ferrar and Byrd glaciers.

(2) In spite of the limited number of occurrences, the petrological study of the AND-2A Ca-amphibole metamorphic clasts reveals the key role of this lithology in the identification of three distinct provenance areas of the present-day segment of the Transantarctic Mountains including the Koettlitz-Blue glacier area in the Royal Society Range, the Mulock-Skelton glacier area, and the Britannia Range. Ca-amphibole compositions and zonations also provide a tool to semiquantitatively estimate P-T conditions attending the formation of metamorphic mineral assemblages in both outcrop and clast sample parageneses. The results of the application of empirical Ca-amphibole geothermobarometry contribute new P and T estimates that are essential for a better understanding of the regional metamorphic patterns and the metamorphic evolution in the three provenance regions. In agreement with literature data, the new results provide further information supporting the coincidence of the three regions with distinct metamorphic terrains showing partly different metamorphic evolutions. Importantly, the data provide the first evidence that intermediate-P medium-grade conditions are documented in the Britannia Range.

(3) Analysis of the down-core distribution of the investigated clasts and combinations of their provenance with clast shape, position in the host lithological units, nature of the main host lithofacies and composition of associated basement clasts provide insight into the depositional processes with a variety of settings from open marine with icebergs to distal, proximal, and subglacial.

(4) The study contributes further evidence that the AND-2A core records two distinct glacial scenarios reflecting either fluctuations with

dominant flows from W to E of local (<100 km from the drill site) paleoglaciers in the Royal Society Range, or fluctuations of ice grounded at the regional scale in the Ross Embayment with flow lines running N-S close to the Transatlantic Mountains front at times for more than 500 km during glacial maxima. Both scenarios further demonstrate the importance of the AND-2A core to reveal a hitherto unavailable, near-field record of dynamic paleoenvironmental history during significant steps in the Antarctic glacial evolution through the Miocene climatic events indicated by proxy records.

## ACKNOWLEDGMENTS

The ANDRILL Program is a multinational collaboration between the Antarctic programs of Germany, Italy, New Zealand, and the United States. Antarctica New Zealand is the project operator and developed the drilling system in collaboration with Alex Pyne at Victoria University of Wellington and Webster Drilling and Exploration Ltd. Antarctica New Zealand supported the drilling team at Scott Base; Raytheon Polar Services Corporation supported the science team at McMurdo Station and the Crary Science and Engineering Laboratory. The ANDRILL Science Management Office at the University of Nebraska-Lincoln provided science planning and operational support. Scientific studies are jointly supported by the U.S. National Science Foundation (NSF), New Zealand Foundation for Research, Science and Technology (FRST), the Italian Antarctic Research Program (PNRA), the German Research Foundation (DFG), and the Alfred Wegener Institute for Polar and Marine Research (AWI). This study was supported with the financial support of the Italian Programma Nazionale di Ricerche in Antartide (PNRA) and PRIN 2008 (F.M. Talarico) grants. The very helpful reviews by R. Carosi and B. Storey are gratefully acknowledged.

## REFERENCES CITED

- Acton, G., Crampton, J., Di Vincenzo, G., Fielding, C.R., Florindo, F., Hannah, M., Harwood, D., Ishman, S., Johnson, K., Jovane, L., Levy, R., Lum, B., Marciano, M.C., Mukasa, S., Ohneiser, C., Olney, M., Riesselman, C., Sagnotti, L., Stefano, C., Strada, E., Taviani, M., Tuzzi, E., Verosub, K.L., Wilson, G.S., Zattin, M., and ANDRILL-SMS Science Team, 2008–2009, Preliminary integrated chronostratigraphy of the AND-2A core, ANDRILL Southern McMurdo Sound project, Antarctica: Terra Antarctica, v. 15, p. 211–220.
- Allibone, A.H., 1992, Low-pressure/high-temperature metamorphism of Koettlitz Group schists, Taylor Valley and upper Ferrar Glacier area, South Victoria Land, Antarctica: New Zealand Journal of Geology and Geophysics, v. 35, p. 115–127, doi: 10.1080/00288306.1992.9514506.
- ANDRILL SMS Science Team, 2010, An integrated age model for the ANDRILL-2A drill core: Eric, Italy, ANDRILL Southern McMurdo Sound Project Science Integration Workshop, Program and Abstracts, 6–11 April 2010, ANDRILL Contribution, v. 16, p. 12–13.
- Barrett, P., 1999, Antarctic climate history over the last 100 million years: Terra Antarctica Reports, v. 3, p. 53–72.
- Barrett, P.J., 1979, Proposed drilling in McMurdo Sound: Memoir of the National Institute of Polar Research, v. 13, Special Issue, p. 231–239.
- Barrett, P.J., 1991, The Devonian to Triassic Beacon Supergroup of the Transantarctic Mountains and correlatives in other parts of Antarctica, in Tingey, R.J., ed., The Geology of Antarctica, Oxford Monographs on

- Geology and Geophysics 17: Oxford, Clarendon Press, p. 120–152.
- Billups, K., and Schrag, D.P., 2002, Paleotemperatures and ice volume of the past 27 Myr revisited with paired Mg/Ca and  $^{18}\text{O}/^{16}\text{O}$  measurements on benthic foraminifera: *Paleoceanography*, v. 17, p. 1003–1013, doi:10.1029/2000PA000567.
- Borg, S.G., DePaolo, D.J., Wendlandt, E.D., and Drake, T.G., 1987, Studies of granites and metamorphic rocks, Byrd Glacier area: *Antarctic Journal of the United States*, v. 24, p. 19–21.
- Brown, E.H., 1977, The crossite content of Ca-amphibole as a guide to pressure of metamorphism: *Journal of Petrology*, v. 18, p. 53–72.
- Bucker, K., and Frey, M., 1994, Petrogenesis of metamorphic rocks: Springer-Verlag Telos, 341 p.
- Carosi, R., Giacomini, F., Talarico, F., and Stump, E., 2007, Geology of the Byrd Glacier Discontinuity (Ross orogen): New survey data from the Britannia Range, Antarctica, in Cooper, A.K., Barrett, P., Stagg, H., Storey, B., Stump, E., Wise, W., and 10th International Symposium on Antarctic Earth Sciences editorial team, eds., *Antarctica: A Keystone in a Changing World*, Online Proceedings of the Tenth International Symposium on Antarctic Earth Sciences: U.S. Geological Survey Open-File Report 2007-1047, Short Research Paper 030, 6 p., doi:10.3133/of2007-1047.srp030.
- Cook, Y.A., and Craw, D., 2001, Amalgamation of disparate crustal fragments in the Walcott Bay-Foster Glacier area, South Victoria Land, Antarctica: *New Zealand Journal of Geology and Geophysics*, v. 44, p. 403–416, doi:10.1080/00288306.2001.9514947.
- Cook, Y.A., and Craw, D., 2002, Neoproterozoic structural slices in the Ross orogen, Skelton Glacier area, South Victoria Land, Antarctica: *New Zealand Journal of Geology and Geophysics*, v. 45, p. 133–143, doi:10.1080/00288306.2002.9514965.
- Cooper, A.K., and Davey, F.J., 1985, Episodic rifting of the Phanerozoic rocks of the Victoria Land basin, western Ross Sea, Antarctica: *Science*, v. 229, p. 1085–1087, doi:10.1126/science.229.4718.1085.
- Cooper, A.F., Worley, B.A., Armstrong, R.A., and Price, R.C., 1997, Synorogenic Alkaline and Carbonatic magmatism in the Transantarctic Mountains of South Victoria Land, Antarctica, in Ricci, C.A., ed., *The Antarctic Region: Siena, Italy, Geological Evolution and Processes*, Terra Antarctica Publications, p. 245–252.
- Cornamusini, G., 2010, Sedimentary coarse clasts in AND-2A core, ANDRILL Southern McMurdo Sound Project, Antarctica: Stratigraphic distribution and provenance: *Erice, Italy, ANDRILL Southern McMurdo Sound Project Science Integration Workshop, Program and Abstracts*, 6–11 April 2010, ANDRILL Contribution, v. 16, p. 22–24.
- Cottle, J.M., 2002, Evolution of a convergent margin - A petrological study of Ross orogeny magmatism in the Carlyn Glacier region, southern Victoria Land, Antarctica [M.S. thesis]: University of Otago Library, 200 p.
- Cottle, J.M., and Cooper, A.F., 2006, Geology, geochemistry and geochronology of an A-type granite in the Mulock Glacier area, southern Victoria Land, Antarctica: *New Zealand Journal of Geology and Geophysics*, v. 49, p. 191–202.
- Cowan, E.A., Hillenbrand, C.-D., Hassler, L.E., and Ake, M.T., 2008, Coarse-grained terrigenous sediment deposition on continental rise drifts: A record of Pliocene glaciation on the Antarctic Peninsula: *Palaeogeography, Palaeoclimatology, Palaeoecology*, v. 265, p. 275–291, doi:10.1016/j.palaeo.2008.03.010.
- Cox, S.C., 1992, Garnet-biotite geothermometry of Koettlitz Group metasediments, Wright Valley, South Victoria Land, Antarctica: *New Zealand Journal of Geology and Geophysics*, v. 35, p. 29–40, doi:10.1080/00288306.1992.9514497.
- Cox, S.C., 1993, Inter-related plutonism and deformation in South Victoria Land, Antarctica: *Geological Magazine*, v. 130, p. 1–14, doi:10.1017/S0016756800023682.
- Craddock, C., 1970, Tectonic map of Gondwana, in Bushnell, V.C., and Craddock, C., eds., *Geological Maps of Antarctica*: New York, American Geographical Society, Antarctic Map Folio Series, Folio 12, plate XXIII.
- Di Vincenzo, G., Bracciali, L., Del Carlo, P., Panter, K., and Rocchi, S., 2010,  $^{40}\text{Ar}$ - $^{39}\text{Ar}$  dating of volcanogenic products from the AND-2A core (ANDRILL Southern McMurdo Sound Project, Antarctica): Correlations with the Erebus Volcanic Province and implications for the age model of the core: *Bulletin of Volcanology*, v. 72, p. 487–505, doi:10.1007/s00445-009-0337-z.
- Drewry, D.J., 1983, Antarctica: Glaciological and geophysical folio: Cambridge, United Kingdom, University of Cambridge, Scott Polar Research Institute, 9 p.
- Ehrmann, W., Setti, M., and Marinoni, L., 2005, Clay minerals in Cenozoic sediments off Cape Roberts (McMurdo Sound, Antarctica) reveal palaeoclimatic history: *Palaeogeography, Palaeoclimatology, Palaeoecology*, v. 229, p. 187–211, doi:10.1016/j.palaeo.2005.06.022.
- Elliott, D.H., 1992, Jurassic magmatism and tectonism associated with Gondwanaland break-up: An Antarctic perspective, in Storey, B.C., Alabaster, T., and Punkhurst, R.J., eds., *Magmatism and the causes of continental break-up*: The Geological Society of London Special Publication 68, p. 165–184.
- Elliott, D.H., Fleming, T.H., Haban, M.A., and Siders, M.A., 1995, Petrology and mineralogy of the Kirkpatrick basalt and Ferrar dolerites, Mesa Range region, north Victoria Land, Antarctica: Contribution to Antarctic Research IV: Antarctic Research Series, v. 67, p. 103–141.
- Fahnestock, M.A., Scambos, T.A., Bindschadler, R.A., and Kvaran, G., 2000, A millennium of variable ice flow recorded by the Ross Ice Shelf, Antarctica: *Journal of Glaciology*, v. 46, p. 652–664, doi:10.3189/172756500781832693.
- Fielding, C.R., Whittaker, J., Henrys, S.A., Wilson, T.J., and Naish, T.R., 2008, Seismic facies and stratigraphy of the Cenozoic succession in McMurdo Sound, Antarctica: Implications for tectonic, climatic and glacial history: *Palaeogeography, Palaeoclimatology, Palaeoecology*, v. 260, p. 8–29, doi:10.1016/j.palaeo.2007.08.016.
- Fielding, C.R., Atkins, C.B., Bassett, K.N., Browne, G.H., Dunbar, G.B., Field, B.D., Frank, T.D., Krissek, L.A., Panter, K.S., Passchier, S., Pekar, S.F., Sandroni, S., Talarico, F., and ANDRILL-SMS Science Team, 2008–2009, Sedimentology and stratigraphy of the AND-2A core, ANDRILL Southern McMurdo Sound project, Antarctica: *Terra Antarctica*, v. 15, p. 77–112.
- Findlay, R.H., Skinner, D.N.B., and Craw, D., 1984, Lithostratigraphy and structure of the Koettlitz Group, McMurdo Sound, Antarctica: *New Zealand Journal of Geology and Geophysics*, v. 27, p. 513–536.
- Florindo, F., Wilson, G.S., Roberts, A.P., Sagnotti, L., and Verosub, K.L., 2005, Magnetostratigraphic chronology of a late Eocene to early Miocene glacial marine succession from the Victoria Land Basin, Ross Sea, Antarctica: *Global and Planetary Change*, v. 45, p. 207–236, doi:10.1016/j.gloplacha.2004.09.009.
- Gerya, T.V., Perchuk, L.L., Triboulet, C., Audren, C., and Sez'ko, A.I., 1997, Petrology of the Tumanshet Zonal Metamorphic Complex, Eastern Sayan: *Petrology*, v. 5, p. 503–533.
- Goode, J.W., 2007, Metamorphism in the Ross orogen and its bearing on Gondwana margin tectonics, in Cloos, M., Carlson, W.D., Gilbert, M.C., Liou, J.G., and Sorensen, S.S., eds., *Convergent Margin Tectonics and Associated Regions: A Tribute to W.G. Ernst*: Geological Society of America Special Paper 419, p. 185–203.
- Goode, J.W., Williams, I.S., and Myrow, P., 2004, Provenance of Neoproterozoic and lower Paleozoic siliciclastic rocks of the central Ross orogen, Antarctica: Detrital record of rift-, passive- and active-margin sedimentation: *Geological Society of America Bulletin*, v. 116, p. 1253–1279, doi:10.1130/B25347.1.
- Gunn, B.M., and Warren, G., 1962, Geology of Victoria Land between the Mawson and Mulock Glaciers, Antarctica: *New Zealand Geological Survey Bulletin*, v. 71, p. 1–157.
- Hambrey, M.J., Barrett, P.J., and Powell, R.D., 2002, Late Oligocene and early Miocene glacial marine sedimentation in the SW Ross Sea, Antarctica: The record from offshore drilling, in Dowdeswell, J.A., and Ó Cofaigh, C., eds., *Glacier-influenced sedimentation on high-latitude continental margins: The Geological Society of London Special Publications*, v. 203, p. 105–128.
- Harwood, D.M., Florindo, F., Talarico, F.M., and Levy, R.H., eds., 2008–2009, Studies from the ANDRILL Southern McMurdo Sound Project, Antarctica: Initial science report on AND-2A: *Terra Antarctica*, v. 15, p. 5–235.
- Holbourn, A., Kuhn, W., Schulz, M., Flores, J.-A., and Andersen, N., 2007, Orbitally-paced climate evolution during the middle Miocene “Monterey” carbon-isotope excursion: *Earth and Planetary Science Letters*, v. 261, p. 534–550, doi:10.1016/j.epsl.2007.07.026.
- Holland, T.J.B., and Richardson, S.W., 1979, Amphibole zonation in metabasites as a guide to the evolution of metamorphic conditions: Contributions to Mineralogy and Petrology, v. 70, p. 143–148, doi:10.1007/BF00374442.
- Kominz, M.A., Browning, J.V., Miller, K.G., Sugarman, P.J., Mizintseva, S., and Scotese, C.R., 2008, Late Cretaceous to Miocene sea-level estimates from the New Jersey and Delaware coastal plain coreholes: An error analysis: *Basin Research*, v. 20, p. 211–226, doi:10.1111/j.1365-2117.2008.00354.x.
- Kretz, R., 1983, Symbols for rock forming minerals: *The American Mineralogist*, v. 68, p. 277–279.
- Kyle, P.R., 1981, Glacial history of the McMurdo Sound area as indicated by the distribution and nature of McMurdo Volcanic Group rocks, in McGinnis, L.D., ed., *Dry Valley Drilling Project, Antarctic Research Series 33*: Washington, D.C., American Geophysical Union, p. 403–412.
- Kyle, P.R., 1990, McMurdo Volcanic Group, western Ross Embayment. Introduction, in Le Masurier, W.E., and Thomson, J.W., eds., *Volcanoes of the Antarctic Plate and Southern Oceans*: American Geophysical Union Antarctic Research Series 48, p. 19–25.
- Leake, B.E., Woolley, A.R., Arps, C.E.S., Birch, W.D., Gilbert, M.C., Grice, J.D., Hawthorne, F.C., Kato, A., Kisch, H.J., Krichovichev, V.G., Linthout, K., Laird, J., Mandarino, J.A., Maresch, W.V., Nickel, E.H., Rock, N.M.S., Schumacher, J.C., Smith, D.C., Stephenson, N.C.N., Ungaretti, L., Whittaker, E.J.W., and Youzhi, G., 1997, Nomenclature of amphiboles: Report of the Subcommittee on Amphiboles of the International Mineralogical Association, Commission on New Minerals and Mineral Names: *The American Mineralogist*, v. 35, p. 219–246.
- Martin, A.P., Cooper, A.F., and Dunlap, W.J., 2010, Geochronology of Mount Morning, Antarctica: Two-phase evolution of a long-lived trachyte-basaltite-phonolite eruptive center: *Bulletin of Volcanology*, v. 72, p. 357–371, doi:10.1007/s00445-009-0319-1.
- Miller, K.G., Mountain, G.S., and the Leg 150 Shipboard Party, Members of the New Jersey Coastal Plain Drilling Project, 1996, Drilling and dating New Jersey Oligocene–Miocene sequences: Ice volume, global sea level, and Exxon records: *Science*, v. 271, p. 1092–1095, doi:10.1126/science.271.5252.1092.
- Miyashiro, A., 1994, *Metamorphic petrology*: London, University College Limited Press, 404 p.
- Naish, T., Powell, R., Levy, R., and the ANDRILL MIS Science Team, 2007, Initial science results from AND-1B, ANDRILL McMurdo Ice Shelf Project, Antarctica: *Terra Antarctica*, v. 14, p. 1–328.
- Panter, K.S., Talarico, F., Bassett, K., Del Carlo, P., Field, B., Frank, T., Hoffmann, S., Kuhn, G., Reichelt, L., Sandroni, S., Taviani, M., Bracciali, M., Cornamusini, G., von Eynatten, H., Rocchi, S., and ANDRILL-SMS Science Team, 2008–2009, Petrologic and geochemical composition of the AND-2A core, ANDRILL Southern McMurdo Sound Project, Antarctica: *Terra Antarctica*, v. 15, p. 147–192.
- Papike, J.J., Cameron, K.C., and Baldwin, K., 1974, Amphiboles and pyroxenes: characterization of other than quadrilateral components and estimate of ferric iron from microprobe data: *Geological Society of America, Abstracts with Programs*, v. 6, p. 1053–1054.
- Passchier, S., Fielding, C.R., Pekar, S., Panter, K., Harwood, D., Browne, G., Field, B., Krissek, L., Falk, C., and Florindo, F., 2010, Facies distribution of AND-2A and implications for ice dynamics during early and middle Miocene Climatic Optima and the middle Miocene climate transition: *Erice, Italy, ANDRILL Southern McMurdo Sound Project Science Integration Workshop, Program and Abstracts*, 6–11 April 2010, ANDRILL Contribution, v. 16, p. 79–81.
- Raase, P., 1974, Al and Ti contents of hornblende, indicators of pressure and temperature of regional metamorphism: Contributions to Mineralogy and Petrology, v. 45, p. 231–236, doi:10.1007/BF00383440.

- Reinardy, B.T.I., Pudsey, C.J., Hillenbrand, C.-D., Murray, T., and Evans, J., 2009, Contrasting sources for glacial and interglacial shelf sediments used to interpret changing ice flow directions in the Larsen Basin, Northern Antarctic Peninsula: *Marine Geology*, v. 266, p. 156–171, doi:10.1016/j.margeo.2009.08.003.
- Rowell, A.J., Rees, M.N., Duebendorfer, E.M., Wallin, E.T., van Schmus, W.R., and Smith, E.I., 1993, An active Neoproterozoic margin: Evidence from the Skelton Glacier area, Transantarctic Mountains: *Journal of the Geological Society*, v. 150, p. 677–682, doi:10.1144/gsjgs.150.4.0677.
- Sandroni, S., and Talarico, F.M., 2011, The record of Miocene climatic events in AND-2A drill core (Antarctica): Insights from provenance analyses of basement clasts: *Global and Planetary Change*, v. 75, p. 31–46, doi:10.1016/j.gloplacha.2010.10.002.
- Smellie, J.L., 1998, Sand grain detrital modes in CRP-1: Provenance variations and influence of Miocene eruptions on the marine record in the McMurdo Sound region: *Terra Antarctica*, v. 5, p. 579–587.
- Spear, F.S., 1980, NaSi-CaAl exchange equilibrium between plagioclase and amphibole: An empirical model: *Contributions to Mineralogy and Petrology*, v. 80, p. 140–146.
- Spear, F.S., 1993, *Metamorphic phase equilibria and pressure-temperature-time paths*: Washington, D. C., Monograph Series 1, Mineralogical Society of America, 799 p.
- Stump, E., 1995, *The Ross orogen of the Transantarctic Mountains*: Cambridge, Cambridge University Press, 284 p.
- Talarico, F.M., and Sandroni, S., 1998, Petrography, mineral chemistry and provenance of basement clasts in the CRP-1 drill core (Victoria Land Basin, Antarctica): *Terra Antarctica*, v. 5, p. 601–610.
- Talarico, F.M., and Sandroni, S., 2009, Provenance signature of the Antarctic Ice Sheets in the Ross Embayment during the late Miocene to early Pliocene: The ANDRILL AND-1B core record: *Global and Planetary Change*, v. 69, p. 103–123, doi:10.1016/j.gloplacha.2009.04.007.
- Talarico, F.M., Findlay, R.H., and Rastelli, N., 2005, Metamorphic evolution of the Koettlitz Group in the Koettlitz-Ferrar glaciers region (southern Victoria Land, Antarctica): *Terra Antarctica*, v. 12, p. 3–23.
- Talarico, F.M., Stump, E., Gootee, B.F., Foland, K.A., Palmeri, R., van Schmus, W.R., Brand, P.K., and Ricci, C.A., 2007, First evidence of “Barrovian”-type metamorphic regime in the Ross orogen of Byrd Glacier area, Central Transantarctic Mountains: *Antarctic Science*, v. 19, p. 451–470, doi:10.1017/S0954102007000594.
- Talarico, F.M., McKay, R.M., Powell, R.D., Sandroni, S., and Naish, T., 2011, Late Cenozoic oscillations of Antarctic ice sheets revealed by provenance of basement clasts and grain detrital modes in ANDRILL core AND-1B: *Global and Planetary Change*, doi:10.1016/j.gloplacha.2009.12.002 (in press).
- Triboulet, C., 1992, The (Na-Ca)amphibole-albite-chlorite-epidote-quartz geothermobarometer in the system S-A-F-M-C-N-H<sub>2</sub>O. 1. An empirical calibration: *Journal of Metamorphic Geology*, v. 10, p. 545–556, doi:10.1111/j.1525-1314.1992.tb00104.x.
- Vernon, R.H., 1976, *Metamorphic processes*: London, Murby; New York, Wiley, 247 p.
- Vernon, R.H., and Clarke, G.L., 2008, *Principles of metamorphic petrology*: Cambridge University Press, 446 p.
- Warren, G., 1969a, *Geology of the Terra Nova Bay-McMurdo Sound area, Victoria Land, Antarctic Map Folio Series 12*: New York, American Geographical Society Geology Sheet 14.
- Warren, G., 1969b, *Geology of the Shackleton Coast, Antarctic Map Folio Series 12*: New York, American Geographical Society Geology Sheet 15.
- Wilson, T.J., 1999, Cenozoic structural segmentation of the Transantarctic rift flank in southern Victoria Land: *Global and Planetary Change*, v. 23, p. 105–127, doi:10.1016/S0921-8181(99)00053-3.
- Wynyard, M., 2004, *Geology of the Cocks Glacier area, Antarctica—A study of neo-Proterozoic metamorphism, deformation and magmatism during the Ross orogeny in South Victoria Land* [M.S. thesis]: University of Otago Library, 178 p.
- You, Y., Huber, M., Müller, D.R., Poulsen, C.J., and Ribbe, J., 2009, Simulation of the middle Miocene climate optimum: Implications for future climate: *Geophysical Research Letters*, v. 36, p. L04702, doi:10.1029/2008GL036571.
- Zattin, M., Talarico, F.M., and Sandroni, S., 2010, Integrated provenance and detrital thermochronology studies in the ANDRILL AND-2A drill core: Late Oligocene–early Miocene exhumation of the Transantarctic Mountains (Southern Victoria Land, Antarctica): *Terra Nova*, v. 22, p. 361–368, doi:10.1111/j.1365-3121.2010.00958.x.
- Zenk, M., and Schulz, B., 2004, Zoned Ca-amphiboles and related P-T evolution in metabasites from the classical Barrovian metamorphic zones in Scotland: *Mineralogical Magazine*, v. 68, p. 769–786, doi:10.1180/0026461046850218.

MANUSCRIPT RECEIVED 25 OCTOBER 2010  
 REVISED MANUSCRIPT RECEIVED 8 MARCH 2011  
 MANUSCRIPT ACCEPTED 18 MARCH 2011



Copyright of Geosphere is the property of Geological Society of America and its content may not be copied or emailed to multiple sites or posted to a listserv without the copyright holder's express written permission. However, users may print, download, or email articles for individual use.